

# Stability of the magnetotail current sheet with normal magnetic field and field-aligned plasma flows

Chen Shi <sup>1</sup>, Anton Artemyev <sup>1</sup>, Marco Velli <sup>1</sup>, Anna Tenerani <sup>2</sup>

<sup>1</sup>Earth, Planetary, and Space Sciences, University of California, Los Angeles, Los Angeles, CA 90095, USA

<sup>2</sup>Department of Physics, The University of Texas at Austin, Austin, TX 78712, USA

## Key Points:

- 1D magnetotail current sheet model with a finite  $B_z$  and plasma flows is developed
- Strong stabilizing effect of  $B_z$  is confirmed for current sheets with field aligned flow
- Field-aligned plasma flows cannot overtake the  $B_z$  stabilizing effect

## Abstract

One of the most important problems of magnetotail dynamics is the substorm onset and the related instability of the magnetotail current sheet. Since the simplest 2D current sheet configuration with monotonic  $B_z$  was proven to be stable to the tearing mode, the focus of the instability investigation moved to more specific configurations, e.g. kinetic current sheets with strong transient ion currents and current sheets with non-monotonic  $B_z$  (local  $B_z$  minima or/and peaks). Stability of the latter current sheet configuration has been studied both within kinetic and fluid approaches, whereas the investigation of the transient ion effects were limited to kinetic models only. This paper aims to provide detailed analysis of stability of a multi-fluid current sheet configuration that mimics current sheets with transient ions. Using the system with two field-aligned ion flows that mimic the effect of pressure non-gyrotropy, we construct 1D current sheet with a finite  $B_z$ . This model describes well recent findings of very thin intense magnetotail current sheets. The stability analysis of this two-ion model confirms the stabilizing effect of finite  $B_z$  and shows that the most stable current sheet is the one with exactly counter-streaming ion flows and zero net flow. Such field-aligned flows may substitute the contribution of the pressure tensor nongyrotropy to the stress balance, but cannot overtake the stabilizing effect of  $B_z$ . Obtained results are discussed in the context of magnetotail dynamical models and spacecraft observations.

## 1 Introduction

The problem of current sheet stability is key for most theories and models of magnetospheric dynamics, because such stability determines magnetic reconnection onset (Yamada et al., 2010; Gonzalez & Parker, 2016) and triggers magnetospheric substorms (Baker et al., 1996; Angelopoulos et al., 2013; Sitnov, Birn, et al., 2019). A short review of investigations of the magnetotail current sheet instability should start from the work by (Laval et al., 1966; Coppi et al., 1966), suggesting that magnetic reconnection results from the tearing mode driven by electron currents. Schindler et al. (1973) and Schindler (1974) showed that in realistic magnetotail configuration the normal magnetic field component  $B_z$  (see sketch in Figure 1) destroys the resonant electron interaction with tearing mode (at least for realistic  $B_z$  magnitudes), so only ions can drive tearing. The inclusion of  $B_z \neq 0$  into self-consistent current sheet models require either consideration of a specific class of exact 2D solutions (see, e.g., Kan (1973) and the most recent generalizations in Yoon and Lui (2005); Vasko et al. (2013)) or weakly-2D (with  $\partial^2/\partial x^2 \ll \partial^2/\partial z^2$ ) solutions (see, e.g., (Schindler, 1972) and the most recent generalizations in (Schindler & Birn, 2002; Birn, Schindler, & Hesse, 2004; Artemyev et al., 2016)). Further investigation of *electron stabilizing effect* due to  $B_z \neq 0$  (Galeev & Zelenyi, 1976; Galeev & Sudan, 1985) reduces the parametric space for instability, whereas the consideration of such weakly-2D current sheet configuration (where  $j_y B_z/c$  tension force is balanced by the plasma pressure gradient  $\partial p/\partial x$ , see sketch in Figure 1) demonstrated that such current sheets are stable (Lembege & Pellat, 1982; Pellat et al., 1991; Quest et al., 1996), with a possible exception of unrealistically stretched field line configurations with extremely small  $B_z$  (Goldstein & Schindler, 1982). To resolve the contradiction between well observed magnetic reconnection in the Earth's magnetotail (e.g., Sergeev et al. (1995); Nagai and Machida (1998); Petrukovich et al. (1998); Angelopoulos et al. (2008)) and theoretical current sheet stability, other models have considered the possibility of the reduction of *electron stabilizing effect* (Kuznetsova & Zelenyi, 1991; Zelenyi et al., 2008) and comprehensive and more general current sheet configurations (Pritchett & Buchner, 1995; Sitnov & Schindler, 2010; Sitnov et al., 2013). The important role in development of such new current sheet models has been played by series of MHD (Birn et al., 1998; Birn, Dorelli, et al., 2004) and kinetic (particle-in-cell) (Pritchett et al., 1991; Pritchett & Coroniti, 1994, 1995) simulations of the thin current sheet formation in the magnetotail. These simulations show formation of non-monotonic  $B_z(x)$  profile with a local  $B_z$  minimum

and inverse  $\partial B_z/\partial x < 0$  gradient. Theoretically the formation of a  $B_z$  minimum in the near-Earth plasma sheet may attribute to the steady earthward convection (Hau et al., 1989). Further investigation of a current sheet with  $\partial B_z/\partial x < 0$  has shown that such current sheet is tearing unstable (Sitnov et al., 2014; Bessho & Bhattacharjee, 2014; Pritchett, 2015; Merkin et al., 2015; Birn et al., 2018). There is also indirect observational evidence for the formation of such current sheet configurations in the near-Earth magnetotail (Sergeev et al., 2018; Angelopoulos et al., 2020). All such theoretical models of current sheet instability utilize the same class of 2D current sheets based on the stress balance  $j_y B_z/c = \partial p/\partial x$  (for review of current sheet models of this class, see (Schindler, 2006; Baumjohann et al., 2007) and references therein). However, as will be discussed below, modern spacecraft observations suggest that magnetotail current sheets may not always belong to this class.

A finite  $B_z$  field in the middle and distant magnetotail current sheet (where magnetic field line curvature does not contribute to the cross-tail pressure balance) requires the plasma pressure gradient  $\partial p/\partial x$  to balance the tension force  $j_y B_z/c$ , whereas the equatorial plasma pressure  $p$  must equal the lobe magnetic field pressure  $B_{lobe}^2/8\pi$  (Baumjohann et al., 1990; Petrukovich et al., 1999) that is fitted by a series of empirical models (Nakai et al., 1991; Shukhtina et al., 2004). These models give  $B_{lobe} \approx 25\text{nT} \cdot (-x/20R_E)^{-1}$ , and the corresponding  $j_y \approx (cB_{lobe}/4\pi B_z) \cdot (\partial B_{lobe}/\partial x)$  is limited to  $\sim 1 - 2 \text{ nA/m}^2$  for radial distances  $x \sim -20R_E$  and realistically small  $B_z \sim 1\text{nT}$ . As such current density amplitudes are much smaller than what is typically observed  $5 - 10 \text{ nA/m}^2$  (Runov et al., 2006; Petrukovich et al., 2015; Vasko et al., 2015; Lu et al., 2019), the stress balance  $j_y B_z/c = \partial p/\partial x$  cannot universally describe the magnetotail equilibrium. If we write down the current sheet thickness  $L_z \approx cB_{lobe}/4\pi j_y$  and length  $L_x \approx (\partial \ln p/\partial x)^{-1}$ , this stress balance gives  $L_x = L_z B_{lobe}/2B_z$ , whereas there are observations of current sheets with  $L_x$  much exceeding this limit (Artemyev et al., 2011, 2015). Empirical reconstructions of the magnetotail configuration during the growth phase of a substorm (i.e., before magnetic reconnection) also demonstrates the existence of very long current sheets, likely with  $L_x \gg L_z B_{lobe}/2B_z$  (Sitnov, Stephens, et al., 2019; Sitnov et al., 2021). Thus, statistical observations at the middle (and distant) magnetotail of intense currents  $j_y \geq 5 - 10 \text{ nA/m}^2$ , indirect  $L_x$  estimates and empirical magnetotail reconstructions suggest that 2D current sheet models with  $j_y B_z/c = \partial p/\partial x$  may not be suitable for investigation of the magnetotail current sheet stability (at least for a significant sample of observed configurations). An exploration of models alternative to the class with  $j_y B_z/c = \partial p/\partial x$  is therefore necessary. This argumentation is not valid for the near-Earth magnetotail where the curvature force can contribute to the cross-sheet (vertical) pressure balance. Investigation of stability of the near-Earth current sheet requires analysis of a fully 2D magnetotail configurations (e.g., Goldstein and Schindler (1982); Schindler (2006)).

Plasma anisotropy (if any) may significantly reduce the tension force  $(1-\Lambda)j_y B_z/c = \partial p/\partial x$  with  $\Lambda = 4\pi(p_{\parallel} - p_{\perp})/B^2$  (Rich et al., 1972; Cowley, 1978), i.e. current sheets at the limit of fire-hose instability ( $\Lambda \rightarrow 1$ ) may be almost 1D (Francfort & Pellat, 1976; Cowley & Pellat, 1979). In particular, two-dimensional MHD equilibrium models have shown that both firehose pressure anisotropy and field-aligned flows may yield more stretched magnetotail configurations (Hau, 1993, 1996). However, ions, mostly contributing to the thermal pressure, are mainly isotropic in the magnetotail current sheet (Wang et al., 2013; Artemyev et al., 2019), whereas parallel anisotropic electrons (Walsh et al., 2011; Artemyev et al., 2014) do not contribute more than  $\Lambda \sim 0.1 - 0.3$  for the absolute majority of current sheets (Artemyev, Angelopoulos, Vasko, et al., 2020). More subtle (less measurable and more complex to be described) with respect to anisotropy, another kinetic effect, pressure non-gyrotropy ( $p_{xz} \neq 0$ ), allows balancing of 1D current sheet magnetic forces  $j_y B_z/c = \partial p_{xz}/\partial z$  (Eastwood, 1972; Burkhart et al., 1992; Pritchett & Coroniti, 1992; Ashour-Abdalla et al., 1996; Mingalev et al., 2007; Mingalev et al., 2018). This effect has been included into the series of kinetic cur-

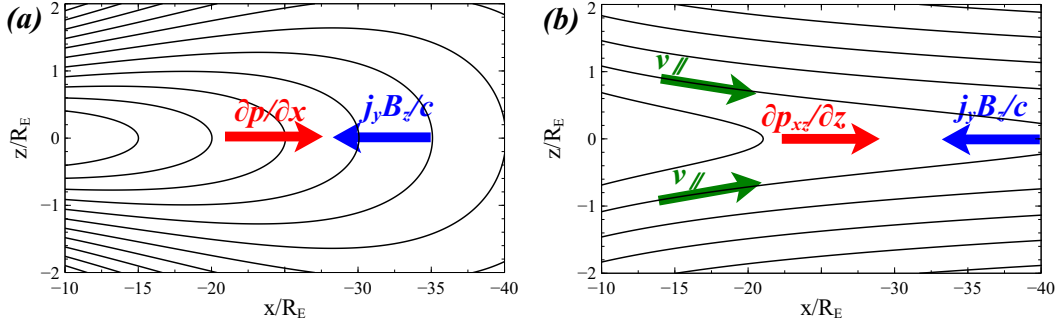


**Figure 1.** Schematic of the magnetotail current sheet configuration: (a) 2D current sheet with the  $j_y B_z / c = \partial p / \partial x$  stress balance, (b) 1D current sheet with  $j_y B_z / c = \partial p_{xz} / \partial z$  stress balance.

rent sheet models (e.g., Sitnov et al. (2003, 2006); Sitnov and Merkin (2016); Zelenyi et al. (2011) and references therein) that can describe many properties of observed current sheets (Artemyev & Zelenyi, 2013). Although direct spacecraft measurements of ion non-gyrotropy in the magnetotail current sheet are quite challenging (see discussion in Zhou et al. (2009); Artemyev et al. (2010, 2019)), such a non-gyrotropy seems to be a prospective solution of the dilemma why magnetotail current sheets are much longer than 2D stress balance limit  $L_x = L_z B_{lobe} / 2B_z$ . Therefore, investigations of stability of 1D current sheets (i.e., current sheet that mimics a  $p_{xz} \neq 0$  effect) should reveal if they are more unstable to tearing mode than the very stable 2D current sheets. This  $p_{xz} \neq 0$  effect is a solution for the 1D current sheet balancing alternative to the balance by the cross-sheet plasma flow. Thus, we consider both these mechanisms of 1D current sheet balance:  $p_{xz} \neq 0$  in absence of cross-sheet bulk flow and strong cross-sheet flow (as in the rotational discontinuity balance).

Although full PIC simulations of 2D current sheet stability (e.g., Pritchett et al. (1991, 1997); Sitnov et al. (2009); Sitnov and Swisdak (2011); Liu et al. (2014); Lu et al. (2018)) have provided many details on the external driver threshold needed to trigger magnetic reconnection, there are almost no investigations of the stability of a 1D nongyrotropic current sheet. To include such investigations into more general context of the tearing instability (Biskamp, 2000; Birn & Priest, 2007), it would be reasonable to start with a fluid resistive model that can reveal a  $B_z$  role in 1D current sheet instability. To mimic the effect of  $p_{xz} \neq 0$  in the stress balance of the fluid current sheet model with  $B_z \neq 0$ , we will adopt multi-fluid model proposed by Steinhauer et al. (2008). In this model two counter-streaming ion flows create  $v_z \partial_z v_x$  terms that balance  $j_y B_z / c$  force with a zero net flow. The generalization of this model would contain imbalanced flows, that is to say a non-zero net flow. This generalization can be then reduced to a single fluid model with the field-aligned flows balancing  $j_y B_z / c$  force, i.e. to the classical rotational discontinuity (Hudson, 1970) with the flow velocity equal to the Alfvén velocity. This paper is devoted to investigation of stability of such generalized 1D multi-fluid model.

The formation and instability of current sheets with stretched magnetic field lines is a common problem in both magnetotail and solar physics (Terasawa et al., 2000; Reeves et al., 2008). In the latter case magnetic reconnection is believed to explain charged particle acceleration and magnetic field energy release in eruptive flares (the so called standard CSHKP model, see Carmichael (1964); Sturrock (1966); Hirayama (1974); Kopp and Pneuman (1976)), non-eruptive events (including, e.g., coalescence of magnetic loops, see Sakai and de Jager (1996)), streamers (e.g., Riley and Luhmann (2012); Edmondson and Lynch (2017); Réville et al. (2020)), and solar wind current sheets (Phan et al., 2006; Gosling, 2012). In contrast to the magnetotail

investigations, mostly focused on the stabilization of the tearing mode by  $B_z$  field, the theory of tearing instability for solar applications is dominated by models of resistive tearing mode in  $B_z = 0$  sheets (e.g., Dobrowolny et al. (1983); Ofman et al. (1991); Loureiro et al. (2012); Tenerani et al. (2015); Del Sarto et al. (2016)). However, the stabilizing effect of  $B_z$  has also been discussed in context of the solar physics (Verneta & Somov, 1987; Somov & Vernet, 1993). Therefore, our investigation of the tearing instability in 1D current sheet with  $B_z \neq 0$  and plasma flows may be of great interests to solar physics applications.

The stress balance in 1D current sheet model with  $B_z \neq 0$  is controlled by counter-streaming plasma flows (see Figure 1(b)), whereas imbalance of these flows results in the net plasma flow across the current sheet. For solar wind plasma such cross-sheet flow is due to current sheet (rotational discontinuity) motion relative to the solar wind (Hudson, 1970; Tsurutani & Ho, 1999). In the Earth's magnetotail there are a couple of mechanisms responsible for formation of such counter-streaming plasma flows. First, formation of thin current sheet is often associated with enhanced precipitations of hot plasma sheet electrons into ionosphere, and these precipitations drive the ionospheric outflow consisting of cold oxygen and hydrogen ions (Keika et al., 2013; Maggiolo & Kistler, 2014; Kronberg et al., 2015). Outflow ions shape fast beams moving along magnetic field lines (Sauvaud et al., 2004; Kistler et al., 2005; Artemyev, Angelopoulos, Runov, & Zhang, 2020) and contributing to the stress balance  $p_{xz}$  (Eastwood, 1972, 1974; Hill, 1975). Although such beams forming in the south and north hemispheres should be generally balanced (i.e., there is a stress balance without a net flow), the precise balance between them is not guaranteed, and there could be a net flow across the current sheet. Second, there are beams of energetic ions moving along plasma sheet boundary layer from the distant magnetotail and coming back to the plasma sheet after reflection from the Earth's dipole field (Ashour-Abdalla et al., 1992, 1996; Grigorenko et al., 2011). These are solar wind protons accelerated in the distant magnetotail by convection (Cowley & Shull, 1983; Ashour-Abdalla et al., 1993; Zelenyi, Dolgonosov, et al., 2006) or reconnection electric fields (Ashour-Abdalla et al., 2006; Grigorenko et al., 2009). Such acceleration mechanisms in combination with Speiser motion (Speiser, 1965; Lyons & Speiser, 1982) shape ion field-aligned beams that contribute significantly to the stress balance in 1D current sheet (Burkhart et al., 1992; Pritchett & Coroniti, 1992; Mingalev et al., 2007). The asymptotic solutions (for infinitely small  $B_z$ ) of such 1D current sheets with counter-streaming plasma flows form a class of models developed in Sitnov et al. (2000) and then generalized by Sitnov et al. (2003, 2006) and (Zelenyi, Malova, et al., 2006; Zelenyi et al., 2011). Models of this class describe bifurcated and embedded current density profiles with properties similar to current sheet properties in the Earth's magnetotail (see model/observation comparison in (Sitnov et al., 2006; Artemyev et al., 2008; Zhou et al., 2009)). The distinguishing feature of these models is the sufficiently long 1D current sheet with the current density magnitude significantly exceeding estimates for 2D isotropic current sheet equilibria,  $c(\partial p/\partial x)/B_z$ . In this study we do not specify particular mechanism of field-aligned plasma flows, and focus on stability of the 1D current sheet model with such flows.

The paper is organized as follows. In Section 2 we present the equations for the zeroth-order equilibrium and the derivation of equations for the perturbed fields. In Section 3, we show the results, i.e. the dispersion relation of the resistive tearing mode, obtained by numerically solving the perturbation equations derived in Section 2. In Section 4 we discuss the results in the context of Earth's magnetosphere. In Section 5 we conclude this study.

## 2 Basic equations

In this section, we present in detail the model of the background field and derivation of the linearized equation set which is solved numerically. The numerical results are presented in Section 3.

### 2.1 Background fields

Incompressibility is assumed throughout the paper such that the plasma density is homogeneous and unperturbed:  $\rho(\mathbf{x}, t) \equiv \rho_0$ . The background magnetic field consists of a Harris-type anti-parallel component and a uniform normal component:

$$\mathbf{B} = B_0 \tanh\left(\frac{z}{a}\right) \hat{e}_x + B_z \hat{e}_z \quad (1)$$

The current density flows along  $y$  across magnetic field lines lying in  $(x, z)$  plane, whereas a field-aligned plasma flow does not change this magnetic field geometry. One can show that  $\nabla \times (\mathbf{B} \cdot \nabla \mathbf{B}) \neq 0$  with this configuration and thus it is impossible to maintain equilibrium with a scalar pressure  $\mathbf{P} = P\mathbf{I}$  solely. As already discussed in Section 1, one simple way to establish equilibrium is introducing the plasma flow such that the shear stress of the flow balances the tension force of the magnetic field. In one-fluid MHD model, an Alfvénic flow  $\mathbf{V} \equiv \mathbf{B}/\sqrt{4\pi\rho}$  is required such that  $\rho\mathbf{V} \cdot \nabla \mathbf{V} \equiv \mathbf{B} \cdot \nabla \mathbf{B}/4\pi$  and the equilibrium is achieved with a uniform total pressure  $P^T = P + B^2/8\pi$ .

We can consider a more generalized case where the protons shape two populations, denoted by subscripts “+” and “-” respectively such that the two corresponding momentum equations are:

$$\rho_{\pm} \mathbf{V}_{\pm} \cdot \nabla \mathbf{V}_{\pm} = -\nabla P_{\pm} + \frac{q}{m_p} \rho_{\pm} \left( \mathbf{E} + \frac{1}{c} \mathbf{V}_{\pm} \times \mathbf{B} \right) \quad (2)$$

where  $\mathbf{E}$  is the electric field,  $q$  is the charge of proton, and  $m_p$  is the proton mass. Sum up the two equations and use the relation  $\mathbf{E} \approx -\mathbf{V}_e \times \mathbf{B}/c$  where  $\mathbf{V}_e$  is the electron flow velocity from the massless and cold electron momentum equation

$$0 = \sum_{\pm} \rho_{\pm} \left( \mathbf{E} + \frac{1}{c} \mathbf{V}_e \times \mathbf{B} \right),$$

we get

$$\rho_+ \mathbf{V}_+ \cdot \nabla \mathbf{V}_+ + \rho_- \mathbf{V}_- \cdot \nabla \mathbf{V}_- = -\nabla \left( P + \frac{B^2}{8\pi} \right) + \frac{1}{4\pi} \mathbf{B} \cdot \nabla \mathbf{B} \quad (3)$$

where  $P = P_+ + P_-$  and we have used the approximation  $\mathbf{J} \approx c\nabla \times \mathbf{B}/4\pi$  where  $\mathbf{J}$  is the electric current density. For convenience we assume  $\rho_+ = \rho_- = \rho/2$ , i.e. the two ion populations are of the same density. Then we write  $\mathbf{V}_{\pm} = \pm\alpha_{\pm} \mathbf{V}_A$  where  $\mathbf{V}_A = \mathbf{B}/\sqrt{4\pi\rho}$  is the magnetic field in Alfvén velocity unit and  $\alpha_{\pm}$  are two constants controlling the speeds of the two ion flows. Apparently we have assumed that both of the two ion populations are streaming along the magnetic field lines. With these assumptions, we get two equilibrium criteria:

$$\frac{d}{dz} \left( P + \frac{B^2}{8\pi} \right) = 0 \quad (4a)$$

$$\left[ 1 - \frac{1}{2} (\alpha_+^2 + \alpha_-^2) \right] B_z \frac{dB_x}{dz} = 0 \quad (4b)$$

Here we note that all the background fields are functions of coordinate  $z$  only. The first equation is the pressure balance condition which constrains the thermal pressure  $P(z)$  and the second equation is the tension force balance condition which leads to the requirement

$$\alpha_+^2 + \alpha_-^2 = 2 \quad (5)$$

Without loss of generality, we assume  $1 \leq \alpha_+ \leq \sqrt{2}$  and thus  $\alpha_- = \pm\sqrt{2 - \alpha_+^2}$ . The positive (+) branch of  $\alpha_-$  corresponds to the case that the two ion flows are counter-streaming and the negative (-) branch of  $\alpha_-$  corresponds to the case that the two ion flows are of the same direction. We define  $\mu = (\alpha_+ - \alpha_-)/2$  such that the average flow speed  $\mathbf{V} = (\mathbf{V}_+ + \mathbf{V}_-)/2 = \mu \mathbf{V}_A$ , i.e.  $\mu = \mathbf{V}/\mathbf{V}_A$  is the amplitude of the average ion velocity normalized by the Alfvén velocity. In Figure 2, we plot the  $\alpha_-(\alpha_+)$  and  $\mu(\alpha_+)$  curves for  $\alpha_+ \in [1, \sqrt{2}]$ . By varying  $\alpha_+$  and selecting either the positive or negative branch of  $\alpha_-$ , we are able to regulate the average flow speed such that  $0 \leq \mu \leq 1$ . Specifically,  $\alpha_+ = \alpha_- = 1$  corresponds to  $\mu = 0$  as in this case the two ion populations are counter-streaming with the same speed  $V_A$ . On the other hand,  $\alpha_{\pm} = \pm 1$  leads to  $\mu = 1$  as in this case the two ion populations are streaming with the same velocity  $\mathbf{V} = \mathbf{V}_A$  and this model converges to the one-fluid MHD model.

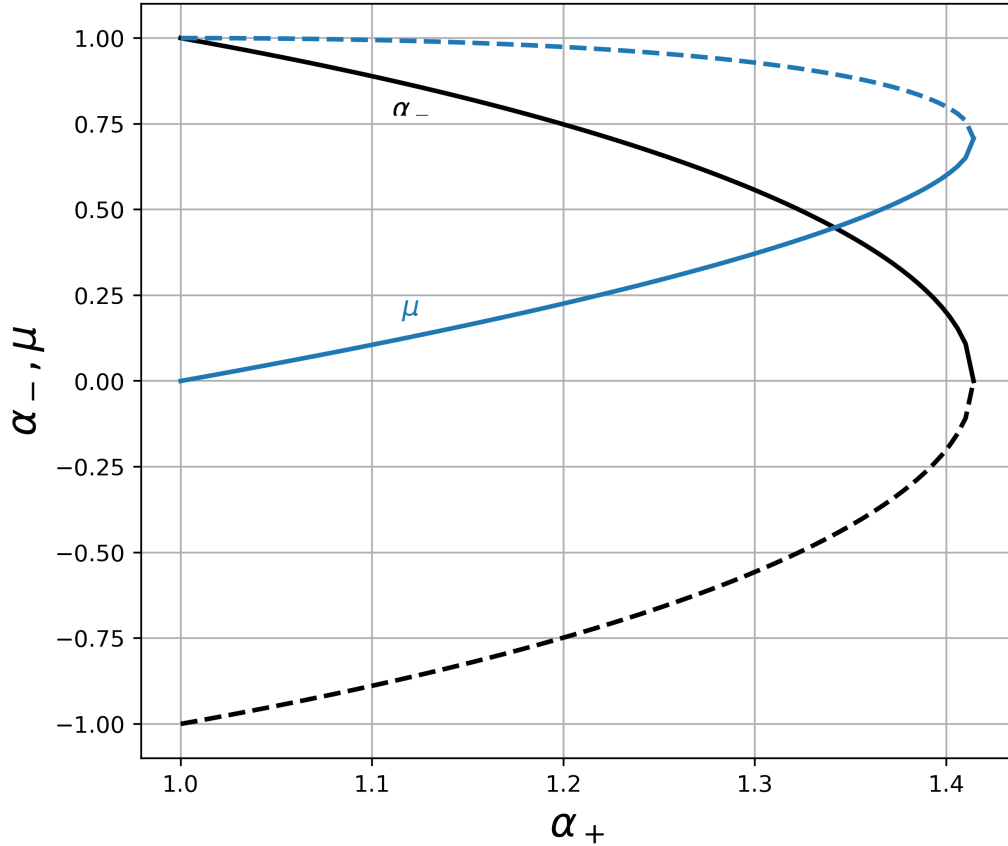


**Figure 2.**  $\alpha_-$  (black) and  $\mu = (\alpha_+ - \alpha_-)/2$  (blue) as functions of  $\alpha_+$ . The dashed segments of the two curves correspond to the negative branch  $\alpha_- = -\sqrt{2 - \alpha_+^2}$ , i.e. the two ion populations flowing in the same direction. The solid segments of the two curves correspond to the positive branch  $\alpha_- = \sqrt{2 - \alpha_+^2}$ , i.e. the two ion populations flowing in the opposite direction.

## 2.2 Perturbation equations

To linearize the equation set, we write the perturbed, or first-order, fields as  $\mathbf{u}_{\pm, e}$ ,  $p_{\pm}$ ,  $\mathbf{b}$ ,  $\mathbf{j}$ , and  $\mathbf{E}_1$  respectively and assume all perturbations are in the form:

$$f(x, z, t) = f(z) \exp(ikx + \gamma t). \quad (6)$$

The linearized momentum equations are:

$$\frac{1}{2}\rho_0 (\gamma \mathbf{u}_\pm + \mathbf{u}_\pm \cdot \nabla \mathbf{V}_\pm + \mathbf{V}_\pm \cdot \nabla \mathbf{u}_\pm) = -\nabla p_\pm + \frac{1}{2} \frac{q}{m_p} \rho_0 \left( \mathbf{E}_1 + \frac{1}{c} \mathbf{u}_\pm \times \mathbf{B} + \frac{1}{c} \mathbf{V}_\pm \times \mathbf{b} \right) \quad (7)$$

where  $\mathbf{E}_1 \approx -\mathbf{u}_e \times \mathbf{B}/c - \mathbf{V}_e \times \mathbf{b}/c$ . For convenience, We further define

$$\mathbf{u} = \frac{1}{2} (\mathbf{u}_+ + \mathbf{u}_-), \mathbf{w} = \frac{1}{2} (\mathbf{u}_+ - \mathbf{u}_-) \quad (8)$$

where  $\mathbf{u}$  is the perturbation of the ion net flow. By adding up and taking difference between the two equations of Eq (7), we get

$$\gamma \mathbf{u} + \mathbf{f}_- \cdot \nabla \mathbf{V}_\mathbf{A} + \mathbf{V}_\mathbf{A} \cdot \nabla \mathbf{f}_- = -\frac{1}{\rho_0} \nabla (p_+ + p_-) + \frac{1}{c\rho_0} (\mathbf{j} \times \mathbf{B} + \mathbf{J} \times \mathbf{b}) \quad (9a)$$

$$\gamma \mathbf{w} + \mathbf{f}_+ \cdot \nabla \mathbf{V}_\mathbf{A} + \mathbf{V}_\mathbf{A} \cdot \nabla \mathbf{f}_+ = -\frac{1}{\rho_0} \nabla (p_+ - p_-) + \frac{q}{m_p c} \left[ \mathbf{w} \times \mathbf{B} + \frac{1}{2} (\alpha_+ + \alpha_-) \mathbf{V}_\mathbf{A} \times \mathbf{b} \right] \quad (9b)$$

where  $\mathbf{f}_\pm = (\alpha_+ \mathbf{u}_+ \pm \alpha_- \mathbf{u}_-)/2$ , and we have used the assumption  $\mathbf{V}_\pm = \pm \alpha_\pm \mathbf{V}_\mathbf{A}$ . If we normalize length to the thickness of the current sheet  $a$ , normalize magnetic field to  $B_0$ , normalize speed to the Alfvén speed  $V_{A0} = B_0/\sqrt{4\pi\rho_0}$ , Eq (9b) becomes:

$$\gamma \mathbf{w} + \mathbf{f}_+ \cdot \nabla \mathbf{B} + \mathbf{B} \cdot \nabla \mathbf{f}_+ = -\nabla (p_+ - p_-) + \frac{a}{d_i} \left[ \mathbf{w} \times \mathbf{B} + \frac{1}{2} (\alpha_+ + \alpha_-) \mathbf{V}_\mathbf{A} \times \mathbf{b} \right] \quad (10)$$

where  $d_i = c/\sqrt{4\pi n e^2/m_p}$  is the ion skin depth and  $n$  is the plasma number density. We can see that, in the MHD limit where the typical length scale  $a$  is much larger than the ion skin depth  $d_i$ , this equation reduces to

$$\mathbf{w} \times \mathbf{B} + \frac{1}{2} (\alpha_+ + \alpha_-) \mathbf{V}_\mathbf{A} \times \mathbf{b} = 0 \quad (11)$$

or alternatively

$$\mathbf{w} = \frac{1}{2} (\alpha_+ + \alpha_-) \mathbf{b} \quad (12)$$

which correlates the magnetic field perturbation and the difference between the perturbations of the two ion flow velocities. In the special case  $\alpha_\pm = \pm 1$ , we have  $\mathbf{w} \equiv 0$ , which is consistent with the fact that the two ion populations merge into one fluid. The induction equation is acquired by inserting  $\mathbf{E}_1 = -\mathbf{u}_e \times \mathbf{B}/c - \mathbf{V}_e \times \mathbf{b}/c + \eta \mathbf{j}$ , where  $\eta$  is the resistivity, into the linearized Maxwell-Faraday equation  $\partial \mathbf{b}/\partial t = -c \nabla \times \mathbf{E}_1$ . As we are analyzing the MHD case and hence the Hall effect is neglected, we can write  $\mathbf{E}_1 \approx -\mathbf{u} \times \mathbf{B}/c - \mathbf{V} \times \mathbf{b}/c + \eta \mathbf{j}$ . After normalization, the linearized induction equation is written as

$$\gamma \mathbf{b} = \mathbf{b} \cdot \nabla \mathbf{V} - \mathbf{V} \cdot \nabla \mathbf{b} + \mathbf{B} \cdot \nabla \mathbf{u} - \mathbf{u} \cdot \nabla \mathbf{B} + \frac{1}{S} \nabla^2 \mathbf{b} \quad (13)$$

where  $S = aV_{A0}/\eta'$  is the Lundquist number and  $\eta' = c^2\eta/4\pi$  is the magnetic diffusivity. Here we have used the divergence-free conditions for both the magnetic field and the flow velocity.

After some algebra starting from Eqs (9a, 12, & 13), a two-equation set for  $u_z$  and  $b_z$  is written as

$$\gamma (u_z'' - k^2 u_z) + \mu \{ B_z (u_z''' - k^2 u_z') + ik [B_x (u_z'' - k^2 u_z) - B_x'' u_z] \} = \sigma \{ B_z (b_z''' - k^2 b_z') + ik [B_x (b_z'' - k^2 b_z) - B_x'' b_z] \} \quad (14a)$$

$$\gamma b_z = (ik B_x u_z + B_z u_z') - \mu (ik B_x b_z + B_z b_z') + \frac{1}{S} (b_z'' - k^2 b_z) \quad (14b)$$

where  $\mu = (\alpha_+ - \alpha_-)/2$ ,  $\sigma = 1 - (\alpha_+ + \alpha_-)^2/4$  and prime indicates  $d/dz$ . From Eq (14), we see that  $B_z$  is a singular parameter as it increases the order of the equation

for  $u_z$  from two to three. In addition, compared with the tearing mode with an anti-parallel magnetic field, the growth rate is in general complex in this model rather than purely real, implying propagating perturbations. It is also worth noting that, if  $B_z = 0$  and  $\alpha_+ = \alpha_- = 0$  such that  $\mu = 0$ ,  $\sigma = 1$ , Eq (14) reduces to the classical tearing mode equation:

$$\gamma (u_z'' - k^2 u_z) = ik [B_x (b_z'' - k^2 b_z) - B_x'' b_z] \quad (15a)$$

$$\gamma b_z = ik B_x u_z + \frac{1}{S} (b_z'' - k^2 b_z) \quad (15b)$$

### 3 Stability analysis

The system of Eq (14) is a boundary-value eigen-problem. The boundary conditions are that  $u_z$  and  $b_z$  vanish far from the current sheet:  $u_z, b_z(z \rightarrow \pm\infty) \rightarrow 0$ . In practice, we cannot set the boundaries to infinity. However, far from the current sheet we have  $B_x \approx \pm B_0$ , i.e.  $B_x$  is approximately constant, so it is observed that  $u_z, b_z \propto \exp(-k|z|)$  are solutions to Eq (14a). Plugging the condition  $u_z, b_z \propto \exp(-k|z|)$  into Eq (14b), we get the ratio between  $u_z$  and  $b_z$  at the boundaries. We use the boundary-value-problem solver implemented in the Python library SciPy (Virtanen et al., 2020) to solve Eq (14). The solver adopts a 4th order collocation algorithm with the control of residuals (ref. Kierzenka & Shampine, 2001; Ascher et al., 1994) and is able to solve the eigenvalue and eigen-functions simultaneously. The solver has been successfully utilized to analyze the linear stability of the oblique tearing mode with a guide field (Shi et al., 2020).

#### 3.1 Effect of $B_z \neq 0$

In Figure 3, we plot the dispersion relations  $\gamma - k$  and  $\omega - k$  in the top (panel (a)) and bottom (panel (b)) panels respectively. We note that, here  $\gamma$  and  $\omega$  are the real and opposite-imaginary parts of the complex  $\gamma$  appearing in Eq (14), i.e.  $\gamma_{complex} = \gamma - i\omega$ . For this figure, the Lundquist number  $S$  is fixed at  $10^4$  and  $\mu$ , i.e. the average ion speed normalized to  $V_{A0}$ , is fixed at 1.0, corresponding to an Alfvénic one-fluid model as discussed in Section 2.1. In each panel, curves of different colors correspond to different values of  $B_z$ , ranging from 0.001 to 0.1. To validate the solver and to testify whether the solution to Eq (14) converges as the singular parameter  $B_z \rightarrow 0$ , we also solve the problem with  $B_z = 0$  at which the equation set degenerates to a lower order. The solved  $\gamma$  and  $\omega$  for  $B_z = 0$  are plotted as dashed curves and we can see that as  $B_z$  approaches to 0 from a finite value, the  $\gamma - k$  curve converges to the dashed one. We note that if  $B_z$  is exactly zero,  $\omega$  is also zero, i.e. the mode is not propagating due to the fact that the background shear flow is symmetric in  $z$ . From panel (a) of Figure 3, we see that the growth rate is monotonically decreasing with  $B_z$ . That is to say, the existence of a finite  $B_z$  quenches the growth of the instability.

In analysis of the tearing instability, how the maximum growth rate scales with the Lundquist number is important. In Figure 4, we show the maximum growth rate  $\gamma_m$ , which is the peak value of each  $\gamma - k$  curve such as those shown in Figure 3, as a function of the Lundquist number  $S$  for  $\mu = 1$  and different values of  $B_z$  in log-log scale. In the figure, squares are the numerical results and solid lines are linear-fittings of the squares. Obviously,  $\gamma_m$  decreases with increasing  $B_z$ , consistent with the results shown in Figure 3. For  $B_z = 0$ , a clear power-law relation  $\gamma_m \propto S^{-0.65}$  is observed. We note that in a current sheet without any flow, the fastest growing tearing mode has a growth rate  $\gamma_m \propto S^{-0.5}$ . Thus, the scaling  $\gamma_m \propto S^{-0.65}$  indicates that the current sheet is more stable with the Alfvénic background flow than without the flow. As we increase  $B_z$ , the  $\gamma_m - S$  line is no longer straight, as can be seen from the curves  $B_z = 0.005$  and  $B_z = 0.01$ , whose slopes gradually transit to  $-1$  at large Lundquist numbers. When  $B_z$  is large enough, i.e.  $B_z = 0.05$  and  $B_z = 0.075$ , the whole  $\gamma_m - S$  curve in the regime  $S \geq 10^3$  is straight with a slope  $-1$ . We note

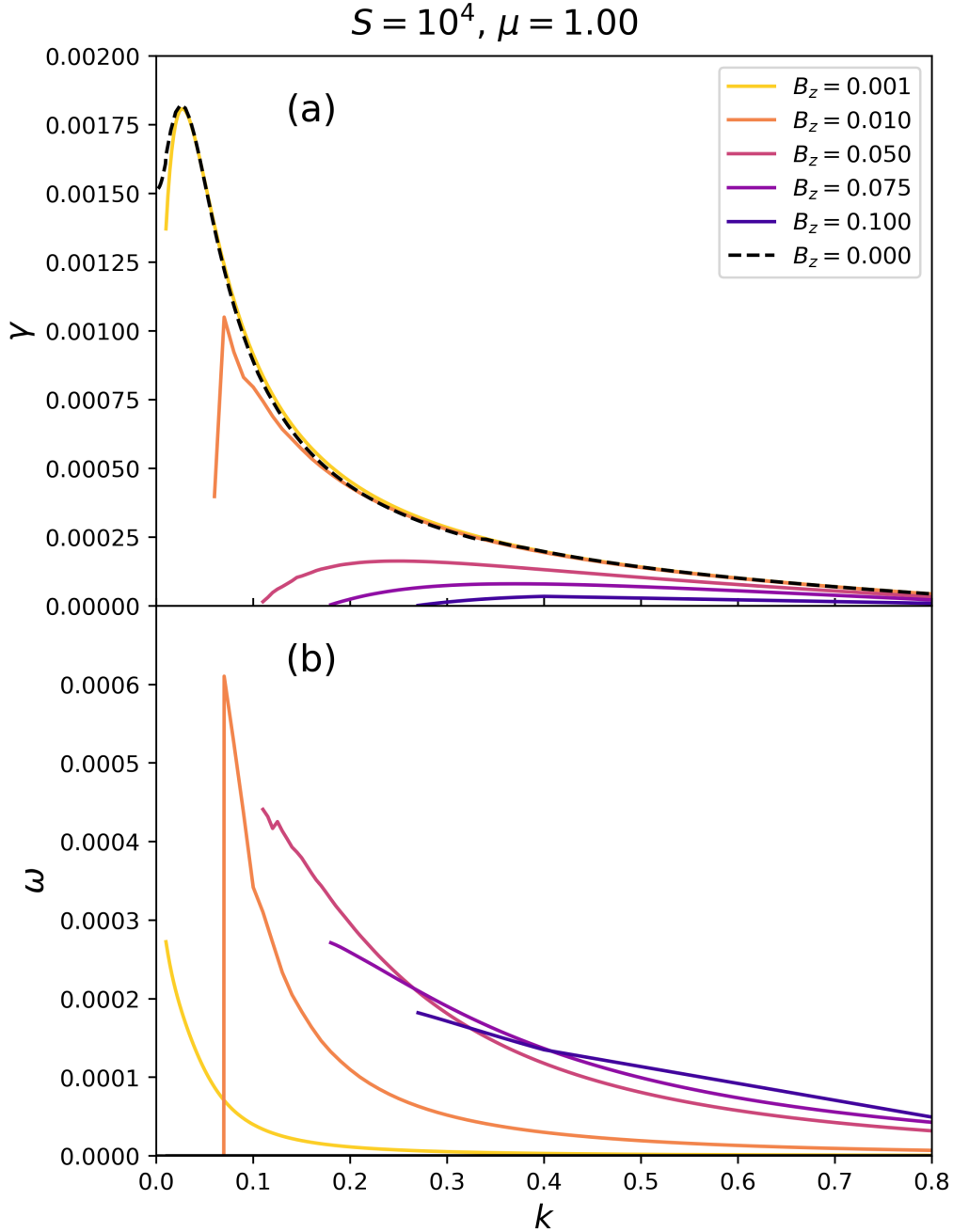


**Figure 3.** (a)  $\gamma - k$  and (b)  $\omega - k$  curves for  $S = 10^4, \mu = 1$ , and varying  $B_z$ . The light (yellow) to dark (purple) colors correspond to  $B_z$  increasing from 0.001 to 0.1. The black dashed curve is  $B_z = 0$ .

that, a growth rate  $\gamma \propto S^{-1}$  implies that  $\gamma \propto \eta/a^2$ , that is to say, there is actually no “growth” of instability in the system because the growth rate is supported purely by the diffusion of the background magnetic field. Thus, Figure 4 shows that, a finite  $B_z$  significantly stabilizes the current sheet: when either  $B_z$  or  $S$  is large enough, the

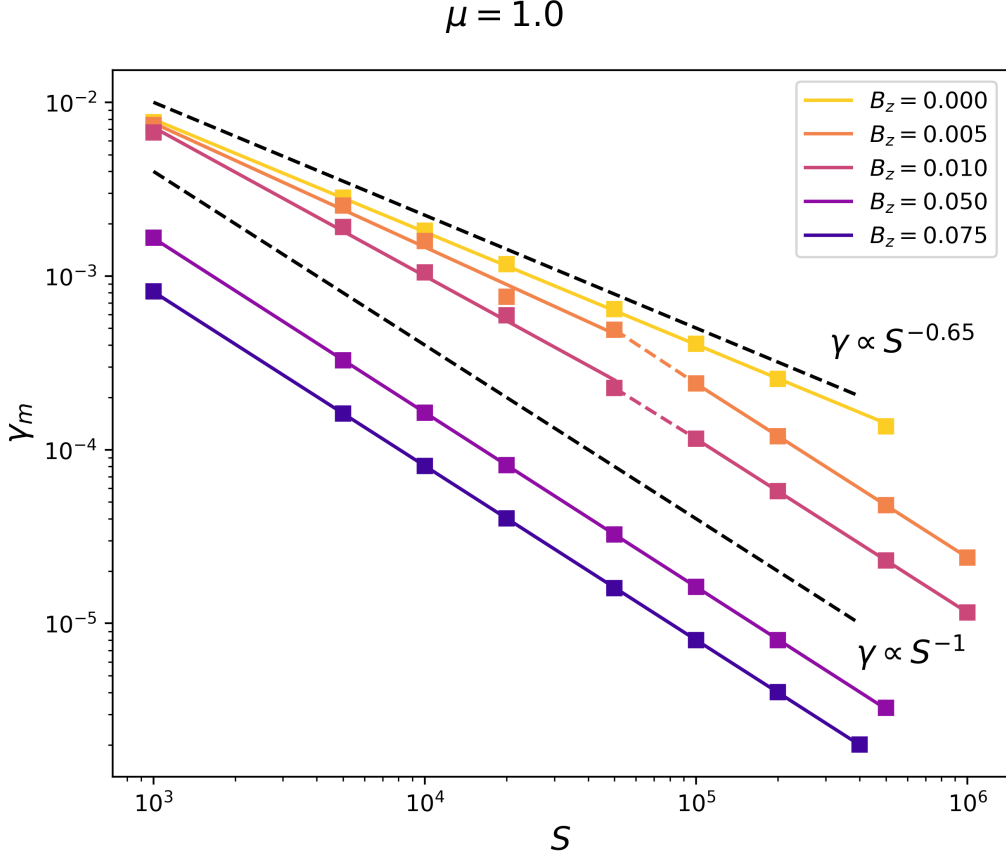


**Figure 4.** Maximum growth rate  $\gamma_m$  as a function of  $S$  for  $\mu = 1$  and varying  $B_z$  in log-log scale. The squares are the numerical results and the solid lines are linear-fittings of the squares. For  $B_z = 0.005$  and  $B_z = 0.01$  we apply a two-segment linear-fitting as the slope of the curve is clearly non-constant. The two black dashed lines are  $\gamma \propto S^{-0.65}$  and  $\gamma \propto S^{-1}$  for reference.

tearing instability vanishes and only the diffusion is taking effect in transferring the energy from the background magnetic field to the perturbed fields.

### 3.2 Effect of $\mu < 1$

In Figure 5, we plot the  $\gamma - k$  (panel (a)) and  $\omega - k$  (panel (b)) curves for  $S = 10^4$ ,  $B_z = 0.01$ , and varying  $\mu$ , i.e. the average ion flow speed. From panel (a), we see that the growth rate decreases with  $\mu$  in general. In Figure 6, we plot the maximum growth rate  $\gamma_m$  as a function of the Lundquist number  $S$  for  $B_z = 0.01$  and different values of  $\mu$  in log-log scale. Apparently, the  $\gamma_m - S$  relation is not a single power law and the  $\gamma_m - S$  curve steepens with  $S$ . Similar to what is shown in Figure 4, for very large  $S$  the relation converges to  $\gamma_m \propto S^{-1}$ , i.e. a status where the instability is merely a result of diffusion.

From Figures 5 & 6, we can see that as  $\mu \rightarrow 0$ , the growth rate converges to zero. This is the case  $\alpha_+ = \alpha_- = 1$  where the two ion populations counter stream at exactly the same speed  $V_{A0}$ . In this case,  $\mu = \sigma = 0$  and Eq (14a) reduces to  $\gamma(u_z'' - k^2 u_z) = 0$ , which naturally gives the solution  $\gamma = 0$  since otherwise we are left with  $u_z'' - k^2 u_z = 0$  which does not have a solution of  $u_z$  that decays to zero at

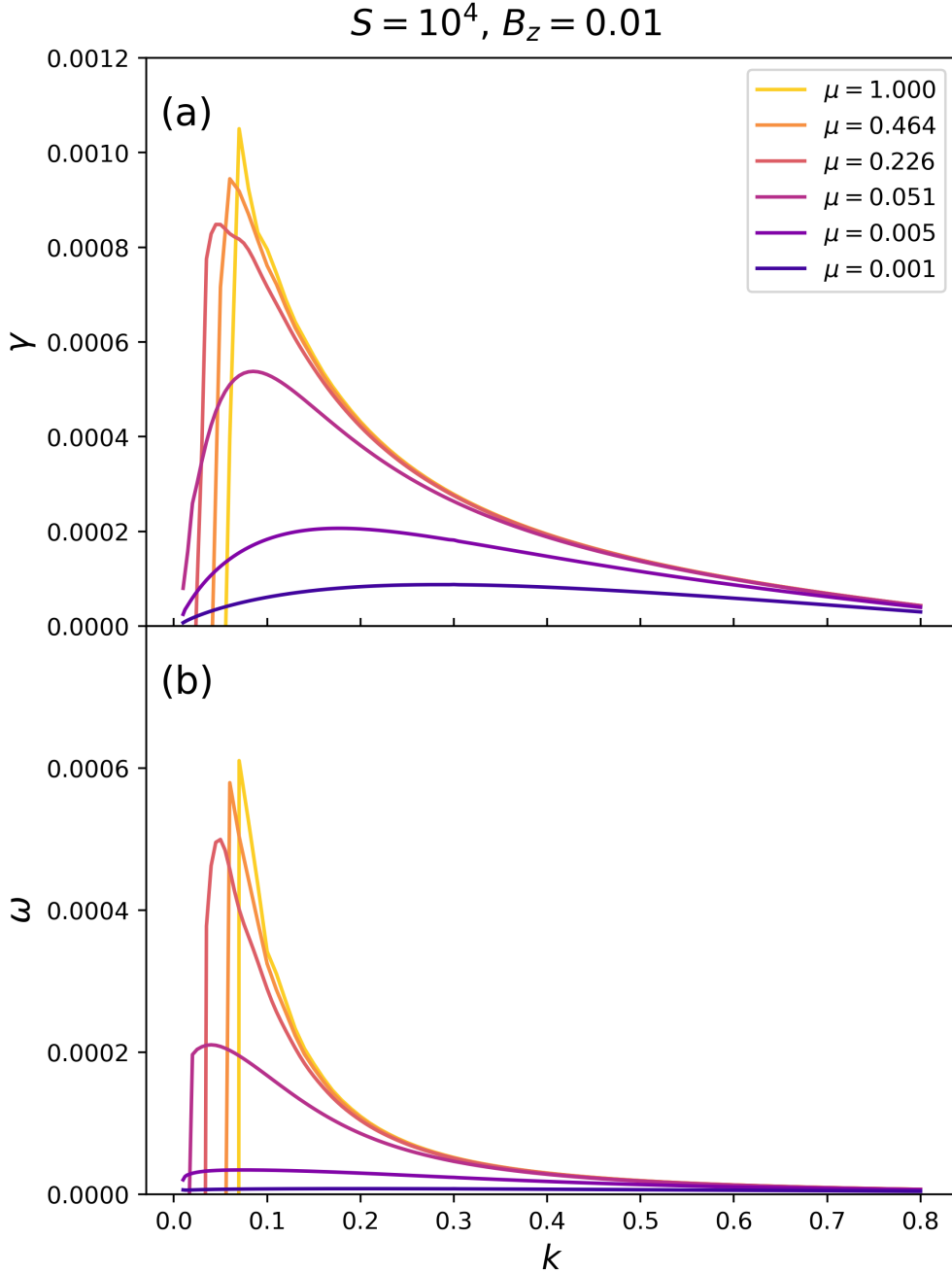


**Figure 5.** (a)  $\gamma - k$  and (b)  $\omega - k$  curves for  $S = 10^4$ ,  $B_z = 0.01$  and varying  $\mu$ . The light (yellow) to dark (purple) colors correspond to  $\mu$  decreasing from 1.0 to 0.001.

$|z| \rightarrow \pm\infty$ . However, we should point out that, the average speed  $\mu$  in this two-proton model is not equivalent to the flow speed in the one-fluid MHD model. Consider the case  $B_z = 0$  so that we are freely to add a one-fluid shear flow of any speed as long as its velocity is parallel to the background magnetic field. In Figure 7, we show the maximum growth rate  $\gamma_m$  as a function of  $S$  for  $B_z = 0$  and different flow speed  $\mu$ .

$$B_z = 0.01$$

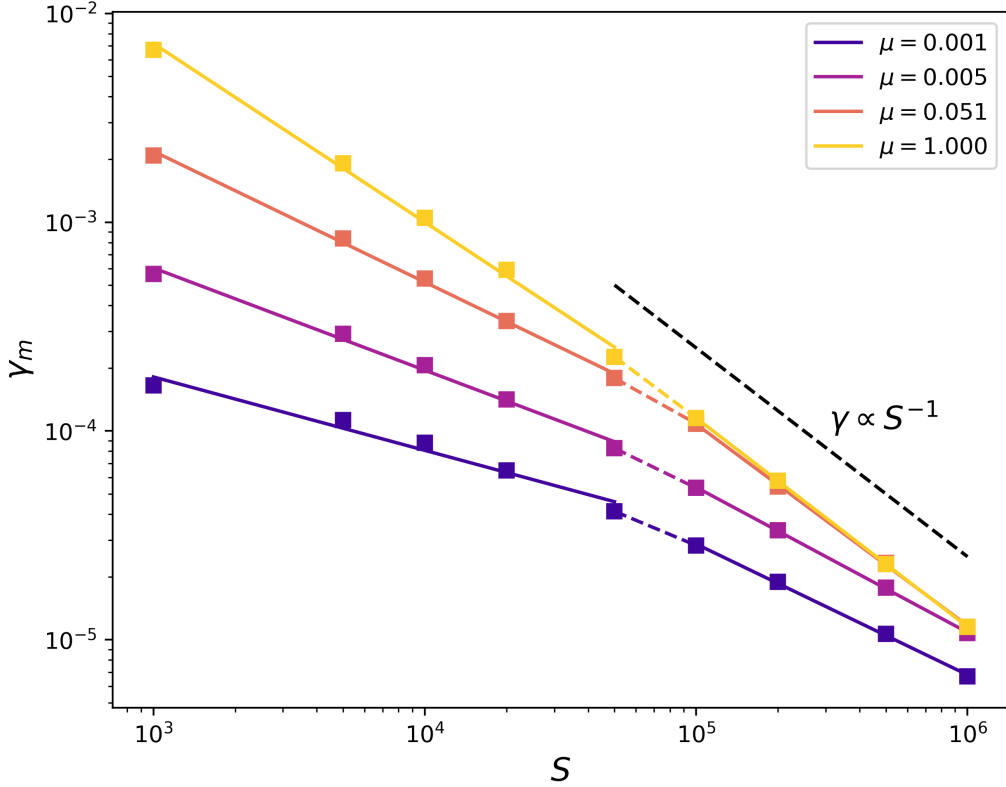


**Figure 6.** Maximum growth rate  $\gamma_m$  as a function of  $S$  for  $B_z = 0.01$  and varying  $\mu$ . The squares are the numerical results and the solid lines are linear-fittings of the squares. The black dashed line is  $\gamma \propto S^{-1}$  for reference.

However, different from Figure 6, the results are calculated based on the one-fluid MHD model, i.e. there is only one proton population. Figure 7 shows that, in the MHD case,  $\gamma_m$  decreases with  $\mu$ , at least for  $\mu \leq 1$  (Chen et al., 1997). For  $\mu > 1$ , the shear flow is super-Alfvénic and thus Kelvin-Helmholtz instability will arise (Wang et al., 1988). Except for  $\mu = 1.0$ ,  $\gamma_m$  scales with  $S$  as  $\gamma_m \propto S^{-0.5}$ . That is to say, although the background flow suppresses the tearing instability, the scaling relation of the maximum growth rate with  $S$  does not change. However, as  $\mu$  approaches unity, the scaling relation changes to  $\gamma_m \propto S^{-0.65}$ , implying that the system becomes more stable, consistent with previous studies ((Dahlburg et al., 1997) and (Einaudi & Rubini, 1986)) which show that the growth rate scales as  $S^{-\beta}$  with  $1/2 < \beta < 2/3$ . But We note here that, these studies claim that in resistive-MHD regime the current sheet with Alfvénic plasma flow (i.e., our  $\mu = 1$  case) is stable. However, our numerical results indicate that this case is not ideally stable but has finite positive growth rate as shown in Figure 3 & 7. In general, we can write  $\gamma_m \tau_a \sim S^{-\beta}$  where  $S = aV_{A0}/\eta$  and  $\tau_a = a/V_{A0}$ . We note that this expression is for a 1D current sheet which is infinitely long. In practice, consider a current sheet of finite length  $L$ , we usually need to measure the time scale by  $\tau_L = L/V_{A0}$  and we define the Lundquist number by  $S_L = LV_{A0}/\eta$ . This transforms the scaling relation to  $\gamma_m \tau_L \sim S_L^{-\beta} (a/L)^{-\beta-1}$ . Apparently, the inverse aspect ratio  $a/L$  is a key parameter determining the growth rate  $\gamma_m \tau_L$ . For an arbitrary

inverse aspect ratio  $a/L \sim S_L^{-\delta}$ , we get  $\gamma_m \tau_L \sim S_L^{-\beta+\delta(\beta+1)}$ , implying a threshold  $\delta = \beta/(\beta+1)$ , at which  $\gamma_m \tau_L \sim O(1)$  is achieved and this is the so-called “ideal tearing” (Pucci & Velli, 2013; Tenerani et al., 2016; Pucci et al., 2020). For the classical tearing  $\beta = 1/2$ , we have  $\delta = 1/3$ , that is to say when a macroscopic current thins to  $a/L \sim S_L^{-1/3}$ , the growth rate of the tearing mode transits from extremely small (assuming  $S_L \rightarrow \infty$ ) to unity and thus the current sheet breaks up rapidly. As  $\beta$  increases, such as in the MHD case with Alfvénic flow shown in Figure 7 or in the two-ion case shown in Figures 4 & 6, the critical value of  $\delta$  also increases, indicating that the current sheet must be thinner in order to achieve fast growth of the tearing instability. For example, for  $\beta \approx 2/3$  as in the Alfvénic flow case, we have  $\delta = 2/5 > 1/3$  and especially, for  $\beta = 1$ , we get the threshold  $a/L \sim S_L^{-1/2}$ , indicating that fast growth of instability happens only when Sweet-Parker type current sheet is formed. This is because, as we discussed before,  $\gamma_m \tau_a \sim S^{-1}$  implies that the growth of instability is fully supported by diffusion.

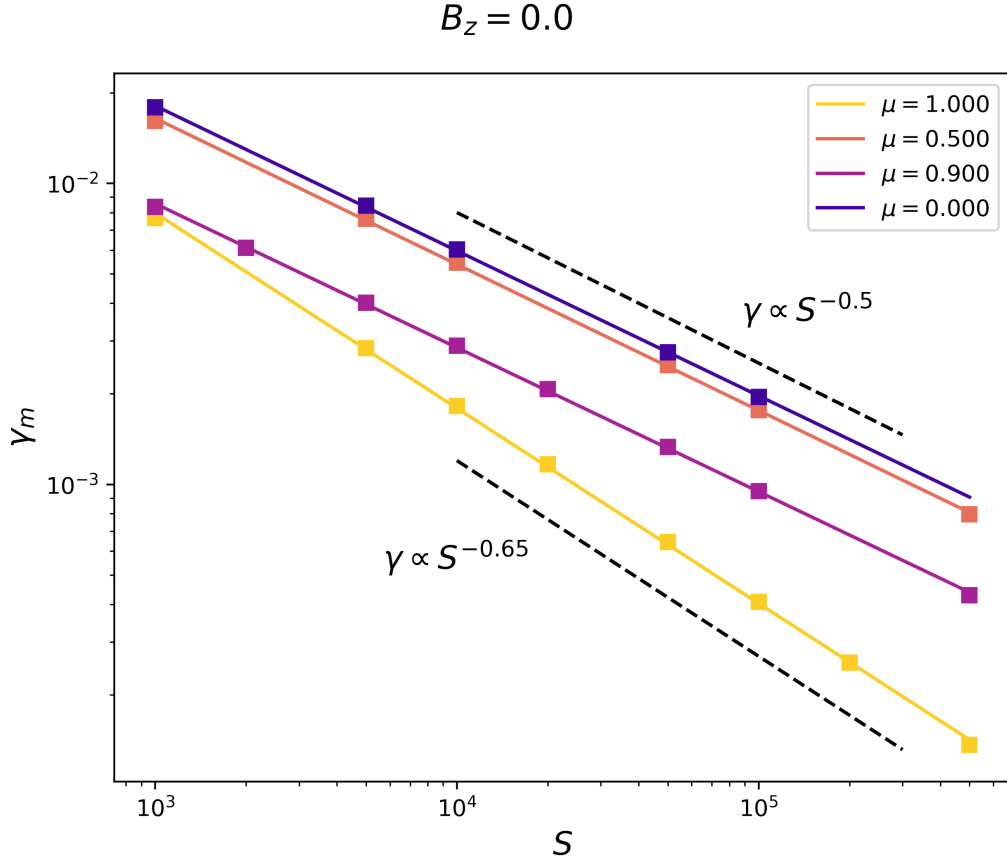


**Figure 7.** Maximum growth rate  $\gamma_m$  as a function of  $S$  for  $B_z = 0$  and varying  $\mu$  based on one-fluid MHD model. The squares are the numerical results and the solid lines are linear-fittings of the squares. The black dashed lines are  $\gamma \propto S^{-0.5}$  and  $\gamma \propto S^{-0.65}$  for reference.

### 3.3 Eigen-functions

In Figure 8, we show the eigen-functions  $u_z$  and  $b_z$  for three sets of parameters. Panel (a) is  $B_z = 0.01$ ,  $\mu = 1.0$ , panel (b) is  $B_z = 0.05$ ,  $\mu = 1.0$ , and panel (c) is

$B_z = 0.01$ ,  $\mu = 0.051$ . The shapes of the eigen-functions do not differ significantly among the three cases, though the relative amplitudes of  $u_z$  and  $b_z$  change with the parameters. The most outstanding feature of these eigen-functions is the quasi-odd function  $b_z(z)$ . It is known that for the classical tearing mode,  $b_z$  is symmetric in  $z$  such that  $b_z(z = 0) > 0$ , which provides the magnetic flux necessary for the reconnection to happen. Meanwhile,  $u_z$  is naturally asymmetric in  $z$  as  $z = 0$  is the stagnation point of the flow. From Figure 8, we can see that  $b_z$  is nearly asymmetric in  $z$  so that  $b_z(z = 0)$  is very small, limiting the reconnection rate. In addition, as the function  $b_z(z)$  is very different from the classical tearing case, plasmoids will not be generated at the center of the current sheet but on the two sides of the the current sheet instead.

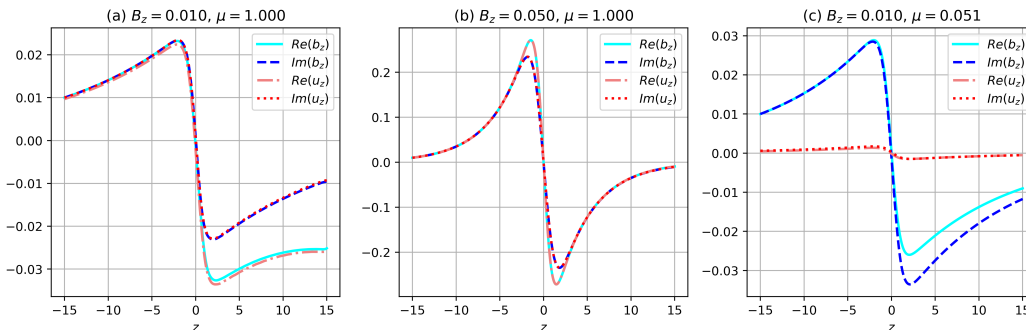


**Figure 8.** Numerically solved eigen-functions  $u_z$  and  $b_z$  for three sets of parameters: (a)  $B_z = 0.01$ ,  $\mu = 1.0$ . (b)  $B_z = 0.05$ ,  $\mu = 1.0$ . (c)  $B_z = 0.01$ ,  $\mu = 0.051$ . Cyan solid curves are the real parts of  $b_z$ , blue dashed curves are the imaginary parts of  $b_z$ , coral dashed-dotted curves are the real parts of  $u_z$ , and red dotted curves are the imaginary parts of  $u_z$ .

## 4 Discussion

In this study we investigate the stability of 1D current sheet with a finite normal component of magnetic field  $B_z \neq 0$  and the tension force  $j_y B_z / c$  balanced by the plasma flows. Two main results are: (1) strong stabilizing effect of  $B_z$  in such 1D current sheets and (2) possible destabilization by imbalance of counter-streaming flows, i.e. by field-aligned net flow. Next, we will discuss these results in the context of the Earth’s magnetotail dynamics.

### 4.1 Current sheet instability at substorm onset

As observations suggest the formation of thin (almost 1D) current sheets during substorm growth phase (Petrukovich et al., 2013; Artemyev et al., 2015; Sitnov et al., 2021), there is a natural interest to investigate the instability of such current sheet configuration. The main idea is that 1D current sheets with nongyrotropic pressure tensor (i.e., with  $B_z j_y / c \approx \partial p_{xz} / \partial z$ ) would be more unstable than classical 2D current sheets (with  $B_z j_y / c \approx \partial p / \partial x$ ), and this resolves the issue of magnetic reconnection onset during weak substorms without strong external drivers (see discussion in Zelenyi et al. (2008)). We use multi-fluid current sheet model with the counter-streaming plasma flows generating such nongyrotropy ( $p_{xz} \neq 0$ ). Our results show that we cannot make current sheet with  $B_z \neq 0$  more unstable solely by substituting  $\partial p / \partial x$  by  $\partial p_{xz} / \partial z$ . This result suggests that the investigation of spontaneous (undriven) instability in the magnetotail current sheet requires more specific current sheet configurations. One of the ideas has been proposed by Sitnov and Schindler (2010) for 2D current sheets

and confirmed in a set of MHD (Merkin et al., 2015; Birn et al., 2018) and kinetic (Sitnov et al., 2014; Bessho & Bhattacharjee, 2014; Pritchett, 2015) simulations which show that current sheets with non-monotonical  $B_z(x)$  profiles can be more unstable. Alternative ideas would be needed to explain spontaneous reconnection in 1D current sheets (with  $B_z = \text{const}$ ), and we showed that such ideas should include more than pressure nongyrotropy.

## 4.2 Field-aligned plasma flows

We generalize the 1D current sheet model of (Steinhauer et al., 2008) by including a net plasma flow. Such flow is shown to be able to reduce the stabilization effect of  $B_z \neq 0$ . This is an interesting effect, because similar field-aligned flows can be included into 2D current sheet equilibria in application to the magnetotail and solar flares (Birn, 1992; Hau, 1996; Nickeler & Wiegmann, 2010). Using an approach proposed by Birn (1991, 1992), one can introduce arbitrary flow along magnetic field lines in a single MHD, and such flow may influence the stability of 2D current sheets, i.e. altering the magnitude of inverse  $\partial B_z / \partial x$  gradient that is considered to destabilize such current sheets (Merkin et al., 2015; Birn et al., 2018). Note, this destabilizing effect of field-aligned plasma flow differs from the stabilizing effect of cross-field diamagnetic flow considered by Swisdak et al. (2003). Indeed, we focus here on the stability conditions of structures with a finite normal component, whereas the (Swisdak et al., 2003) model and its observational confirmations (Phan et al., 2010, 2014) were obtained for much more unstable tangential discontinuities without a normal component  $B_n$ . Our results show that current sheets with  $B_n \neq 0$  and plasma flow equal to the Alfvén speed are completely stable to tearing, and can therefore survive for a long time, e.g., during the long lasting substorm growth phase. The same result explains the absence of magnetic reconnection signatures in multiple rotational discontinuities observed in the near-Sun region (Phan et al., 2020).

Obtained results generalize the previous investigations of the plasma flow effects on the current sheet instability in the absence of  $B_z$ , i.e. for 1D tangential discontinuities with 1D (Chen et al., 1997; Wang et al., 1988; Hoshino & Higashimori, 2015) and 2D plasma flows (Phan & Sonnerup, 1991; Ip & Sonnerup, 1996). The effect of decrease of the growth rate for the long wavelength tearing mode due to the sub-Alfvénic plasma flow, found for such tangential discontinuities (Bulanov et al., 1978), has been revealed for the 1D current sheet with  $B_z \neq 0$ . However, contrast to generally stabilizing effect of the sub-Alfvénic plasma flow on the tearing more in tangential discontinuity (Dahlburg et al., 1997; Einaudi & Rubini, 1986), in the current sheet with  $B_z \neq 0$  the field-aligned flow increases the peak growth rate, i.e. the most stable current sheet with  $B_z \neq 0$  is formed by two counter-streaming flows, whereas any imbalance between these two flows provide an additional free energy for the tearing mode. This effect resembles the effect of super-Alfvénic flow driving the tearing mode in the tangential discontinuities (Wang et al., 1988).

## 4.3 Speculation on possible drivers of magnetic reconnection in the magnetotail

Our results show that 1D current sheet, such as ones formed at the late stage of the substorm growth phase, is well stable relative to the tearing mode. Together with results of 2D current sheet stability (see discussion in Sitnov et al. (2002)), our results rise the question of initialization of substorm reconnection in absence of strong external driver (i.e. spontaneous reconnection). One of the solutions of this issue has been proposed by (Sitnov & Schindler, 2010; Sitnov et al., 2013) for 2D current sheets with nonmonotonical  $B_z(x)$  profiles. This solution has been shown to work for current sheets with  $\partial p / \partial x = B_z j_y / c$ , and one of the prospective directions of further investigation is the merging of models of such 2D current sheets and current sheet with field-aligned

plasma flows. Inclusion of such flows (in multi-fluid approach) will relax  $\partial p/\partial x = B_z j_y/c$  condition by addition  $\partial p_{xz}/\partial z$  term, and thus realistic quasi-1D current sheets with a weak  $\partial p/\partial x$  can be described. From other point of view, even weak  $\partial p/\partial x$  allows inclusion of a nonmonotonical  $B_z(x)$  profiles as a possible source of free energy for the tearing mode. Another prospective approach consists further generalization of multi-fluid models with inclusion of realistic anisotropic electron components (see discussion in Artemyev, Angelopoulos, Vasko, et al. (2020)). Intense electron currents in high-beta plasma of thin current sheets may provide an additional free energy source for the tearing mode excitation.

## 5 Conclusions

In this work, we carried out linear stability analysis of the 1D MHD current sheet with a uniform normal magnetic field ( $B_z$  in the magnetotail coordinates). In our model, the magnetic tension force is balanced by the field-aligned ion flow, which is generalized by assuming that ions shape two populations of the same density but with different field-aligned velocities. The main results of our calculation are

1. The existence of a finite  $B_z$  significantly stabilizes the tearing instability. With a finite  $B_z$ , the scaling relation between the maximum growth rate of the instability ( $\gamma_m$ ) and the Lundquist number ( $S$ ) converges to  $\gamma_m \propto S^{-1}$  in the limit  $S \rightarrow \infty$ , indicating the instability is purely diffusion-supported.
2. In this two-ion model, the most stable case is when the two ion populations counter-stream at the same speed  $V = B/\sqrt{4\pi\rho}$  such that the net flow velocity is zero. In this case the instability does not grow at all. An imbalance between the two ion populations, which lead to a non-zero net flow, destabilizes the current sheet. The most unstable case is when the two ion populations stream in the same direction at the same speed  $V = B/\sqrt{4\pi\rho}$ . This is the one-fluid MHD case where the average flow velocity is  $\mathbf{B}/\sqrt{4\pi\rho}$ .

Our results show that, in the magnetotail, a 1D, i.e. very long and thin, current sheet which has a finite  $B_z$  component is very stable to the tearing instability. To answer the question of the onset of fast spontaneous reconnection in the magnetotail, more ingredients are required, such as the ion/electron kinetic effects.

## Acknowledgments

This work was supported by the NASA HERMES DRIVE Science Center grant No. 80NSSC20K0604. The boundary-value-problem solver used in this study can be found at <https://docs.scipy.org/doc/scipy> and is described in (Virtanen et al., 2020).

## References

- Angelopoulos, V., Artemyev, A., Phan, T. D., & Miyashita, Y. (2020, January). Near-Earth magnetotail reconnection powers space storms. *Nature Physics*, *16*(3), 317-321. doi: 10.1038/s41567-019-0749-4
- Angelopoulos, V., McFadden, J. P., Larson, D., Carlson, C. W., Mende, S. B., Frey, H., ... Kepko, L. (2008, August). Tail Reconnection Triggering Substorm Onset. *Science*, *321*, 931-935. doi: 10.1126/science.1160495
- Angelopoulos, V., Runov, A., Zhou, X. Z., Turner, D. L., Kiehas, S. A., Li, S. S., & Shinohara, I. (2013). Electromagnetic Energy Conversion at Reconnection Fronts. *Science*, *341*, 1478-1482. doi: 10.1126/science.1236992
- Artemyev, A. V., Angelopoulos, V., Runov, A., & Zhang, X. J. (2020, July). Ionospheric Outflow During the Substorm Growth Phase: THEMIS Observations of Oxygen Ions at the Plasma Sheet Boundary. *Journal of Geophysical Re-*

- search (*Space Physics*), 125(7), e27612. doi: 10.1029/2019JA027612
- Artemyev, A. V., Angelopoulos, V., Vasko, I. Y., Petrukovich, A. A., Runov, A., Saito, Y., ... Strangeway, R. J. (2020). Contribution of anisotropic electron current to the magnetotail current sheet as a function of location and plasma conditions. *Journal of Geophysical Research: Space Physics*, 125(1), e2019JA027251. Retrieved from <https://agupubs.onlinelibrary.wiley.com/doi/abs/10.1029/2019JA027251> (e2019JA027251 10.1029/2019JA027251) doi: 10.1029/2019JA027251
- Artemyev, A. V., Angelopoulos, V., Vasko, I. Y., Zhang, X. J., Runov, A., & Zelenyi, L. M. (2019, May). Ion Anisotropy in Earth's Magnetotail Current Sheet: Multicomponent Ion Population. *Journal of Geophysical Research (Space Physics)*, 124(5), 3454-3467. doi: 10.1029/2019JA026604
- Artemyev, A. V., Petrukovich, A. A., Nakamura, R., & Zelenyi, L. M. (2010, December). Proton velocity distribution in thin current sheets: Cluster observations and theory of transient trajectories. *J. Geophys. Res.*, 115, A12255. doi: 10.1029/2010JA015702
- Artemyev, A. V., Petrukovich, A. A., Nakamura, R., & Zelenyi, L. M. (2015, May). Two-dimensional configuration of the magnetotail current sheet: THEMIS observations. *Geophys. Res. Lett.*, 42, 3662-3667. doi: 10.1002/2015GL063994
- Artemyev, A. V., Petrukovich, A. A., Zelenyi, L. M., Malova, H. V., Popov, V. Y., Nakamura, R., ... Apatenkov, S. (2008, September). Comparison of multi-point measurements of current sheet structure and analytical models. *Annales Geophysicae*, 26, 2749-2758.
- Artemyev, A. V., Vasko, I. Y., Angelopoulos, V., & Runov, A. (2016, September). Effects of electron pressure anisotropy on current sheet configuration. *Physics of Plasmas*, 23(9), 092901. doi: 10.1063/1.4961926
- Artemyev, A. V., Walsh, A. P., Petrukovich, A. A., Baumjohann, W., Nakamura, R., & Fazakerley, A. N. (2014, September). Electron pitch angle/energy distribution in the magnetotail. *J. Geophys. Res.*, 119, 7214-7227. doi: 10.1002/2014JA020350
- Artemyev, A. V., & Zelenyi, L. M. (2013). Kinetic Structure of Current Sheets in the Earth Magnetotail. *Space Sci. Rev.*, 178, 419-440. doi: 10.1007/s11214-012-9954-5
- Artemyev, A. V., Zelenyi, L. M., Petrukovich, A. A., & Nakamura, R. (2011, July). Hot electrons as tracers of large-scale structure of magnetotail current sheets. *Geophys. Res. Lett.*, 38, L14102. doi: 10.1029/2011GL047979
- Ascher, U. M., Mattheij, R. M., & Russell, R. D. (1994). *Numerical solution of boundary value problems for ordinary differential equations* (Vol. 13). Siam.
- Ashour-Abdalla, M., Berchem, J. P., Buechner, J., & Zelenyi, L. M. (1993, April). Shaping of the magnetotail from the mantle - Global and local structuring. *J. Geophys. Res.*, 98, 5651-5676. doi: 10.1029/92JA01662
- Ashour-Abdalla, M., Frank, L. A., Paterson, W. R., Perroomian, V., & Zelenyi, L. M. (1996, February). Proton velocity distributions in the magnetotail: Theory and observations. *J. Geophys. Res.*, 101, 2587-2598. doi: 10.1029/95JA02539
- Ashour-Abdalla, M., Leboeuf, J. N., Schriver, D., Bosqued, J., Cornilleau-Wehrlin, N., Sotnikov, V., ... Fazakerley, A. N. (2006, October). Instabilities driven by ion shell distributions observed by Cluster in the midaltitude plasma sheet boundary layer. *J. Geophys. Res.*, 111, 10223. doi: 10.1029/2005JA011490
- Ashour-Abdalla, M., Zelenyi, L. M., Bosqued, J. M., & Kovrazhkin, R. A. (1992, March). Precipitation of fast ion beams from the plasma sheet boundary layer. *Geophys. Res. Lett.*, 19, 617-620. doi: 10.1029/92GL00048
- Baker, D. N., Pulkkinen, T. I., Angelopoulos, V., Baumjohann, W., & McPherron, R. L. (1996, June). Neutral line model of substorms: Past results and present view. *J. Geophys. Res.*, 101, 12975-13010. doi: 10.1029/95JA03753
- Baumjohann, W., Paschmann, G., & Luehr, H. (1990, January). Pressure balance

- between lobe and plasma sheet. *Geophys. Res. Lett.*, *17*, 45-48. doi: 10.1029/GL017i001p00045
- Baumjohann, W., Roux, A., Le Contel, O., Nakamura, R., Birn, J., Hoshino, M., ... Runov, A. (2007, June). Dynamics of thin current sheets: Cluster observations. *Annales Geophysicae*, *25*, 1365-1389.
- Bessho, N., & Bhattacharjee, A. (2014, October). Instability of the current sheet in the Earth's magnetotail with normal magnetic field. *Physics of Plasmas*, *21*(10), 102905. doi: 10.1063/1.4899043
- Birn, J. (1991, February). Stretched three-dimensional plasma equilibria with field-aligned flow. *Physics of Fluids B*, *3*(2), 479-484. doi: 10.1063/1.859891
- Birn, J. (1992, November). Quasi-steady current sheet structures with field-aligned flow. *J. Geophys. Res.*, *97*(A11), 16817-16826. doi: 10.1029/92JA01527
- Birn, J., Dorelli, J. C., Hesse, M., & Schindler, K. (2004, February). Thin current sheets and loss of equilibrium: Three-dimensional theory and simulations. *J. Geophys. Res.*, *109*, 2215. doi: 10.1029/2003JA010275
- Birn, J., Hesse, M., & Schindler, K. (1998, April). Formation of thin current sheets in space plasmas. *J. Geophys. Res.*, *103*, 6843-6852. doi: 10.1029/97JA03602
- Birn, J., Merkin, V. G., Sitnov, M. I., & Otto, A. (2018, May). MHD Stability of Magnetotail Configurations With a  $B_z$  Hump. *J. Geophys. Res.*, *123*, 3477-3492. doi: 10.1029/2018JA025290
- Birn, J., & Priest, E. R. (2007). *Reconnection of magnetic fields : magnetohydrodynamics and collisionless theory and observations* (Birn, J. & Priest, E. R., Ed.).
- Birn, J., Schindler, K., & Hesse, M. (2004, February). Thin electron current sheets and their relation to auroral potentials. *J. Geophys. Res.*, *109*, 2217. doi: 10.1029/2003JA010303
- Biskamp, D. (2000). *Magnetic Reconnection in Plasmas*.
- Bulanov, S. V., Syrovatskiĭ, S. I., & Sakai, J. (1978, August). Stabilizing influence of plasma flow on dissipative tearing instability. *Soviet Journal of Experimental and Theoretical Physics Letters*, *28*, 177-179.
- Burkhart, G. R., Drake, J. F., Dusenbery, P. B., & Speiser, T. W. (1992, September). A particle model for magnetotail neutral sheet equilibria. *J. Geophys. Res.*, *97*, 13799-13815. doi: 10.1029/92JA00495
- Carmichael, H. (1964). A Process for Flares. *NASA Special Publication*, *50*, 451-456.
- Chen, Q., Otto, A., & Lee, L. (1997). Tearing instability, kelvin-helmholtz instability, and magnetic reconnection. *Journal of Geophysical Research: Space Physics*, *102*(A1), 151-161.
- Coppi, B., Laval, G., & Pellat, R. (1966, June). Dynamics of the Geomagnetic Tail. *Physical Review Letters*, *16*, 1207-1210. doi: 10.1103/PhysRevLett.16.1207
- Cowley, S. W. H. (1978, November). The effect of pressure anisotropy on the equilibrium structure of magnetic current sheets. *Planetary and Space Science*, *26*, 1037-1061. doi: 10.1016/0032-0633(78)90028-4
- Cowley, S. W. H., & Pellat, R. (1979, March). A note on adiabatic solutions of the one-dimensional current sheet problem. *Planetary Space Science*, *27*, 265-271. doi: 10.1016/0032-0633(79)90069-2
- Cowley, S. W. H., & Shull, P., Jr. (1983, February). Current sheet acceleration of ions in the geomagnetic tail and the properties of ion bursts observed at the lunar distance. *Planetary and Space Science*, *31*, 235-245. doi: 10.1016/0032-0633(83)90058-2
- Dahlburg, R., Boncinelli, P., & Einaudi, G. (1997). The evolution of plane current-vortex sheets. *Physics of Plasmas*, *4*(5), 1213-1226.
- Del Sarto, D., Pucci, F., Tenerani, A., & Velli, M. (2016, March). "Ideal" tearing and the transition to fast reconnection in the weakly collisional MHD and EMHD regimes. *Journal of Geophysical Research (Space Physics)*, *121*(3),

- 1857-1873. doi: 10.1002/2015JA021975
- Dobrowolny, M., Veltri, P., & Mangeney, A. (1983, June). Dissipative instabilities of magnetic neutral layers with velocity shear. *Journal of Plasma Physics*, *29*(3), 393-407. doi: 10.1017/S0022377800000854
- Eastwood, J. W. (1972, October). Consistency of fields and particle motion in the ‘Speiser’ model of the current sheet. *Planetary and Space Science*, *20*, 1555-1568. doi: 10.1016/0032-0633(72)90182-1
- Eastwood, J. W. (1974, December). The warm current sheet model, and its implications on the temporal behaviour of the geomagnetic tail. *Planetary and Space Science*, *22*, 1641-1668. doi: 10.1016/0032-0633(74)90108-1
- Edmondson, J. K., & Lynch, B. J. (2017, November). Formation and Reconnection of Three-dimensional Current Sheets with a Guide Field in the Solar Corona. *Astrophys. J.*, *849*(1), 28. doi: 10.3847/1538-4357/aa83ba
- Einaudi, G., & Rubini, F. (1986). Resistive instabilities in a flowing plasma: I. inviscid case. *The Physics of fluids*, *29*(8), 2563–2568.
- Francfort, P., & Pellat, R. (1976, August). Magnetic merging in collisionless plasmas. *Geophys. Res. Lett.*, *3*, 433-436. doi: 10.1029/GL003i008p00433
- Galeev, A. A., & Sudan, R. N. (1985). *Handbook of plasma physics. Vol. 2: Basic plasma physics II*.
- Galeev, A. A., & Zelenyi, L. M. (1976, June). Tearing instability in plasma configurations. *Soviet Journal of Experimental and Theoretical Physics*, *43*, 1113.
- Goldstein, H., & Schindler, K. (1982, May). Large-Scale Collision-Free Instability of Two-Dimensional Plasma Sheets. *Physical Review Letters*, *48*, 1468-1471. doi: 10.1103/PhysRevLett.48.1468
- Gonzalez, W., & Parker, E. (2016). *Magnetic Reconnection* (Vol. 427). doi: 10.1007/978-3-319-26432-5
- Gosling, J. T. (2012, November). Magnetic Reconnection in the Solar Wind. *Space Sci. Rev.*, *172*, 187-200. doi: 10.1007/s11214-011-9747-2
- Grigorenko, E. E., Hoshino, M., Hirai, M., Mukai, T., & Zelenyi, L. M. (2009, March). “Geography” of ion acceleration in the magnetotail: X-line versus current sheet effects. *J. Geophys. Res.*, *114*, 3203. doi: 10.1029/2008JA013811
- Grigorenko, E. E., Zelenyi, L. M., Dolgonosov, M. S., Artemiev, A. V., Owen, C. J., Sauvaud, J.-A., ... Hirai, M. (2011, December). Non-adiabatic Ion Acceleration in the Earth Magnetotail and Its Various Manifestations in the Plasma Sheet Boundary Layer. *Space Sci. Rev.*, *164*, 133-181. doi: 10.1007/s11214-011-9858-9
- Hau, L.-N. (1993, April). Anisotropic magnetotail equilibrium and convection. *Geophys. Res. Lett.*, *20*, 555-558. doi: 10.1029/93GL00243
- Hau, L. N. (1996, March). General formulation and exact solution for two-dimensional field-aligned magnetohydrodynamic equilibrium flows. *Physics of Plasmas*, *3*(3), 1113-1119. doi: 10.1063/1.871767
- Hau, L. N., Wolf, R. A., Voigt, G. H., & Wu, C. C. (1989, February). Steady state magnetic field configurations for the Earth’s magnetotail. *J. Geophys. Res.*, *94*(A2), 1303-1316. doi: 10.1029/JA094iA02p01303
- Hill, T. W. (1975, December). Magnetic merging in a collisionless plasma. *J. Geophys. Res.*, *80*, 4689-4699. doi: 10.1029/JA080i034p04689
- Hirayama, T. (1974, February). Theoretical Model of Flares and Prominences. I: Evaporating Flare Model. *Solar Phys.*, *34*, 323-338. doi: 10.1007/BF00153671
- Hoshino, M., & Higashimori, K. (2015, May). Generation of Alfvénic waves and turbulence in reconnection jets. *J. Geophys. Res.*, *120*, 3715-3727. doi: 10.1002/2014JA020520
- Hudson, P. D. (1970, November). Discontinuities in an anisotropic plasma and their identification in the solar wind. *Planetary Space Science*, *18*, 1611-1622. doi: 10.1016/0032-0633(70)90036-X

- Ip, J. T. C., & Sonnerup, B. U. Ö. (1996, October). Resistive tearing-mode instability in a magnetic-field-reversing current sheet with coplanar viscous stagnation-point flow. *Journal of Plasma Physics*, *56*(2), 265-284. doi: 10.1017/S0022377800019267
- Kan, J. R. (1973). On the structure of the magnetotail current sheet. *J. Geophys. Res.*, *78*, 3773-3781. doi: 10.1029/JA078i019p03773
- Keika, K., Kistler, L. M., & Brandt, P. C. (2013, July). Energization of O<sup>+</sup> ions in the Earth's inner magnetosphere and the effects on ring current buildup: A review of previous observations and possible mechanisms. *Journal of Geophysical Research (Space Physics)*, *118*, 4441-4464. doi: 10.1002/jgra.50371
- Kierzenka, J., & Shampine, L. F. (2001). A bvp solver based on residual control and the matlab pse. *ACM Transactions on Mathematical Software (TOMS)*, *27*(3), 299-316.
- Kistler, L. M., Mouikis, C., Möbius, E., Klecker, B., Sauvaud, J. A., RéMe, H., ... Balogh, A. (2005, June). Contribution of nonadiabatic ions to the cross-tail current in an O<sup>+</sup> dominated thin current sheet. *J. Geophys. Res.*, *110*, 6213. doi: 10.1029/2004JA010653
- Kopp, R. A., & Pneuman, G. W. (1976, October). Magnetic reconnection in the corona and the loop prominence phenomenon. *Solar Phys.*, *50*, 85-98. doi: 10.1007/BF00206193
- Kronberg, E. A., Grigorenko, E. E., Haaland, S. E., Daly, P. W., Delcourt, D. C., Luo, H., ... Dandouras, I. (2015, May). Distribution of energetic oxygen and hydrogen in the near-Earth plasma sheet. *Journal of Geophysical Research (Space Physics)*, *120*, 3415-3431. doi: 10.1002/2014JA020882
- Kuznetsova, M. M., & Zelenyi, L. M. (1991, October). Magnetic reconnection in collisionless field reversals - The universality of the ion tearing mode. *Geophys. Res. Lett.*, *18*, 1825-1828. doi: 10.1029/91GL02245
- Laval, G., Pellat, R., & Vuillemin, M. (1966). Instabilités électromagnétiques des plasmas sans collisions (CN-21/71). In *Plasma physics and controlled nuclear fusion research, volume ii* (p. 259-277).
- Lembege, B., & Pellat, R. (1982, November). Stability of a thick two-dimensional quasineutral sheet. *Physics of Fluids*, *25*, 1995-2004. doi: 10.1063/1.863677
- Liu, Y.-H., Birn, J., Daughton, W., Hesse, M., & Schindler, K. (2014, December). Onset of reconnection in the near magnetotail: PIC simulations. *J. Geophys. Res.*, *119*, 9773-9789. doi: 10.1002/2014JA020492
- Loureiro, N. F., Samtaney, R., Schekochihin, A. A., & Uzdensky, D. A. (2012, April). Magnetic reconnection and stochastic plasmoid chains in high-Lundquist-number plasmas. *Physics of Plasmas*, *19*(4), 042303-042303. doi: 10.1063/1.3703318
- Lu, S., Artemyev, A. V., Angelopoulos, V., Lin, Y., Zhang, X. J., Liu, J., ... Strangeway, R. J. (2019, Feb). The Hall Electric Field in Earth's Magnetotail Thin Current Sheet. *Journal of Geophysical Research (Space Physics)*, *124*(2), 1052-1062. doi: 10.1029/2018JA026202
- Lu, S., Pritchett, P. L., Angelopoulos, V., & Artemyev, A. V. (2018, Jan). Magnetic reconnection in Earth's magnetotail: Energy conversion and its earthward-tailward asymmetry. *Physics of Plasmas*, *25*(1), 012905. doi: 10.1063/1.5016435
- Lyons, L. R., & Speiser, T. W. (1982, April). Evidence for current sheet acceleration in the geomagnetic tail. *J. Geophys. Res.*, *87*, 2276-2286. doi: 10.1029/JA087iA04p02276
- Maggiolo, R., & Kistler, L. M. (2014, April). Spatial variation in the plasma sheet composition: Dependence on geomagnetic and solar activity. *Journal of Geophysical Research (Space Physics)*, *119*, 2836-2857. doi: 10.1002/2013JA019517
- Merkin, V. G., Sitnov, M. I., & Lyon, J. G. (2015, March). Evolution of gener-

- alized two-dimensional magnetotail equilibria in ideal and resistive MHD. *J. Geophys. Res.*, *120*, 1993-2014. doi: 10.1002/2014JA020651
- Mingalev, O. V., Malova, H. V., Mingalev, I. V., Mel'nik, M. N., Setsko, P. V., & Zelenyi, L. M. (2018, Oct 01). Model of a thin current sheet in the earth's magnetotail with a kinetic description of magnetized electrons. *Plasma Physics Reports*, *44*(10), 899-919. Retrieved from <https://doi.org/10.1134/S1063780X18100082> doi: 10.1134/S1063780X18100082
- Mingalev, O. V., Mingalev, I. V., Malova, K. V., & Zelenyi, L. M. (2007, November). Numerical simulations of plasma equilibrium in a one-dimensional current sheet with a nonzero normal magnetic field component. *Plasma Physics Reports*, *33*, 942-955. doi: 10.1134/S1063780X07110062
- Nagai, T., & Machida, S. (1998). Magnetic Reconnection in the Near-Earth Magnetotail. *Washington DC American Geophysical Union Geophysical Monograph Series*, *105*, 211. doi: 10.1029/GM105p0211
- Nakai, H., Kamide, Y., & Russell, C. T. (1991, April). Influences of solar wind parameters and geomagnetic activity on the tail lobe magnetic field - A statistical study. *J. Geophys. Res.*, *96*, 5511-5523. doi: 10.1029/90JA02361
- Nickeler, D. H., & Wiegmann, T. (2010, August). Thin current sheets caused by plasma flow gradients in space and astrophysical plasma. *Annales Geophysicae*, *28*, 1523-1532. doi: 10.5194/angeo-28-1523-2010
- Ofman, L., Chen, X. L., Morrison, P. J., & Steinolfson, R. S. (1991, June). Resistive tearing mode instability with shear flow and viscosity. *Physics of Fluids B*, *3*(6), 1364-1373. doi: 10.1063/1.859701
- Pellat, R., Coroniti, F. V., & Pritchett, P. L. (1991, February). Does ion tearing exist? *Geophys. Res. Lett.*, *18*, 143-146. doi: 10.1029/91GL00123
- Petrukovich, A. A., Artemyev, A. V., Nakamura, R., Panov, E. V., & Baumjohann, W. (2013, September). Cluster observations of dBz/dx during growth phase magnetotail stretching intervals. *J. Geophys. Res.*, *118*, 5720-5730. doi: 10.1002/jgra.50550
- Petrukovich, A. A., Artemyev, A. V., Vasko, I. Y., Nakamura, R., & Zelenyi, L. M. (2015). Current sheets in the Earth magnetotail: plasma and magnetic field structure with Cluster project observations. *Space Sci. Rev.*, *188*, 311-337. doi: 10.1007/s11214-014-0126-7
- Petrukovich, A. A., Mukai, T., Kokubun, S., Romanov, S. A., Saito, Y., Yamamoto, T., & Zelenyi, L. M. (1999, March). Substorm-associated pressure variations in the magnetotail plasma sheet and lobe. *J. Geophys. Res.*, *104*, 4501-4514. doi: 10.1029/98JA02418
- Petrukovich, A. A., Sergeev, V. A., Zelenyi, L. M., Mukai, T., Yamamoto, T., Kokubun, S., ... Sandahl, I. (1998, January). Two spacecraft observations of a reconnection pulse during an auroral breakup. *J. Geophys. Res.*, *103*, 47-60. doi: 10.1029/97JA02296
- Phan, T., Bale, S., Eastwood, J., Lavraud, B., Drake, J., Oieroset, M., ... others (2020). Parker solar probe in situ observations of magnetic reconnection exhausts during encounter 1. *The Astrophysical Journal Supplement Series*, *246*(2), 34.
- Phan, T. D., Drake, J. F., Shay, M. A., Gosling, J. T., Paschmann, G., Eastwood, J. P., ... Angelopoulos, V. (2014, October). Ion bulk heating in magnetic reconnection exhausts at Earth's magnetopause: Dependence on the inflow Alfvén speed and magnetic shear angle. *Geophys. Res. Lett.*, *41*, 7002-7010. doi: 10.1002/2014GL061547
- Phan, T. D., Gosling, J. T., Davis, M. S., Skoug, R. M., Oieroset, M., Lin, R. P., ... Balogh, A. (2006, January). A magnetic reconnection X-line extending more than 390 Earth radii in the solar wind. *Nature*, *439*, 175-178. doi: 10.1038/nature04393
- Phan, T. D., Gosling, J. T., Paschmann, G., Pasma, C., Drake, J. F., Oieroset, M.,

- ... Davis, M. S. (2010, August). The Dependence of Magnetic Reconnection on Plasma  $\beta$  and Magnetic Shear: Evidence from Solar Wind Observations. *Astrophys. J. Lett.*, 719(2), L199-L203. doi: 10.1088/2041-8205/719/2/L199
- Phan, T. D., & Sonnerup, B. U. Ö. (1991, December). Resistive tearing-mode instability in a current sheet with equilibrium viscous stagnation-point flow. *Journal of Plasma Physics*, 46(3), 407-421. doi: 10.1017/S0022377800016214
- Pritchett, P. L. (2015, June). Instability of current sheets with a localized accumulation of magnetic flux. *Physics of Plasmas*, 22(6), 062102. doi: 10.1063/1.4921666
- Pritchett, P. L., & Buchner, J. (1995, March). Collisionless reconnection in configurations with a minimum in the equatorial magnetic field and with magnetic shear. *J. Geophys. Res.*, 100, 3601-3611. doi: 10.1029/94JA03028
- Pritchett, P. L., & Coroniti, F. V. (1992, November). Formation and stability of the self-consistent one-dimensional tail current sheet. *J. Geophys. Res.*, 97, 16773-16787. doi: 10.1029/92JA01550
- Pritchett, P. L., & Coroniti, F. V. (1994, July). Convection and the formation of thin current sheets in the near-Earth plasma sheet. *Geophys. Res. Lett.*, 21, 1587-1590. doi: 10.1029/94GL01364
- Pritchett, P. L., & Coroniti, F. V. (1995, December). Formation of thin current sheets during plasma sheet convection. *J. Geophys. Res.*, 100, 23551-23566. doi: 10.1029/95JA02540
- Pritchett, P. L., Coroniti, F. V., & Pellat, R. (1997). Convection-driven reconnection and the stability of the near-Earth plasma sheet. *Geophys. Res. Lett.*, 24, 873-876. doi: 10.1029/97GL00672
- Pritchett, P. L., Coroniti, F. V., Pellat, R., & Karimabadi, H. (1991, July). Collisionless reconnection in two-dimensional magnetotail equilibria. *J. Geophys. Res.*, 96, 11. doi: 10.1029/91JA01094
- Pucci, F., & Velli, M. (2013). Reconnection of quasi-singular current sheets: the “ideal” tearing mode. *The Astrophysical Journal Letters*, 780(2), L19.
- Pucci, F., Velli, M., Shi, C., Singh, K., Tenerani, A., Alladio, F., ... others (2020). Onset of fast magnetic reconnection and particle energization in laboratory and space plasmas. *Journal of Plasma Physics*, 86(6).
- Quest, K. B., Karimabadi, H., & Brittnacher, M. (1996, January). Consequences of particle conservation along a flux surface for magnetotail tearing. *J. Geophys. Res.*, 101, 179-184. doi: 10.1029/95JA02986
- Reeves, K. K., Guild, T. B., Hughes, W. J., Korreck, K. E., Lin, J., Raymond, J., ... Wiltberger, M. (2008, September). Posteruptive phenomena in coronal mass ejections and substorms: Indicators of a universal process? *J. Geophys. Res.*, 113, 0. doi: 10.1029/2008JA013049
- Réville, V., Velli, M., Rouillard, A. P., Lavraud, B., Tenerani, A., Shi, C., & Strugarek, A. (2020, May). Tearing Instability and Periodic Density Perturbations in the Slow Solar Wind. *Astrophys. J. Lett.*, 895(1), L20. doi: 10.3847/2041-8213/ab911d
- Rich, F. J., Vasyliunas, V. M., & Wolf, R. A. (1972). On the Balance of Stresses in the Plasma Sheet. *J. Geophys. Res.*, 77, 4670-4676. doi: 10.1029/JA077i025p04670
- Riley, P., & Luhmann, J. G. (2012, April). Interplanetary Signatures of Unipolar Streamers and the Origin of the Slow Solar Wind. *Solar Phys.*, 277(2), 355-373. doi: 10.1007/s11207-011-9909-0
- Runov, A., Sergeev, V. A., Nakamura, R., Baumjohann, W., Apatenkov, S., Asano, Y., ... Balogh, A. (2006, March). Local structure of the magnetotail current sheet: 2001 Cluster observations. *Annales Geophysicae*, 24, 247-262.
- Sakai, J.-I., & de Jager, C. (1996, July). Solar Flares and Collisions Between Current-Carrying Loops Types and Mechanisms of Solar Flares and Coronal Loop Heating. *Space Sci. Rev.*, 77, 1-192. doi: 10.1007/BF00227866

- Sauvaud, J. A., Louarn, P., Fruit, G., Stenuit, H., Vallat, C., Dandouras, J., . . . McCarthy, M. (2004, Jan). Case studies of the dynamics of ionospheric ions in the Earth's magnetotail. *Journal of Geophysical Research (Space Physics)*, *109*(A1), A01212. doi: 10.1029/2003JA009996
- Schindler, K. (1972). A Self-Consistent Theory of the Tail of the Magnetosphere. In B. M. McCormac (Ed.), *Earth's magnetospheric processes* (Vol. 32, p. 200).
- Schindler, K. (1974). A theory of the substorm mechanism. *J. Geophys. Res.*, *79*, 2803-2810. doi: 10.1029/JA079i019p02803
- Schindler, K. (2006). *Physics of Space Plasma Activity* (Schindler, K., Ed.). Cambridge University Press. doi: 10.2277/0521858976
- Schindler, K., & Birn, J. (2002, August). Models of two-dimensional embedded thin current sheets from Vlasov theory. *J. Geophys. Res.*, *107*, 1193. doi: 10.1029/2001JA000304
- Schindler, K., Pfirsch, D., & Wobig, H. (1973, December). Stability of two-dimensional collision-free plasmas. *Plasma Physics*, *15*, 1165-1184. doi: 10.1088/0032-1028/15/12/001
- Sergeev, V. A., Angelopoulos, V., Mitchell, D. G., & Russell, C. T. (1995, October). In situ observations of magnetotail reconnection prior to the onset of a small substorm. *J. Geophys. Res.*, *100*(A10), 19121-19134. doi: 10.1029/95JA01471
- Sergeev, V. A., Gordeev, E. I., Merkin, V. G., & Sitnov, M. I. (2018, March). Does a Local B-Minimum Appear in the Tail Current Sheet During a Substorm Growth Phase? *Geophys. Res. Lett.*, *45*, 2566-2573. doi: 10.1002/2018GL077183
- Shi, C., Velli, M., Pucci, F., Tenerani, A., & Innocenti, M. E. (2020). Oblique tearing mode instability: guide field and hall effect. *The Astrophysical Journal*, *902*(2), 142.
- Shukhtina, M., Dmitrieva, N., & Sergeev, V. (2004, March). Quantitative magnetotail characteristics for different magnetospheric states. *Annales Geophysicae*, *22*, 1019-1032. doi: 10.5194/angeo-22-1019-2004
- Sitnov, M. I., Birn, J., Ferdousi, B., Gordeev, E., Khotyaintsev, Y., Merkin, V., . . . Zhou, X. (2019, Jun). Explosive Magnetotail Activity. *Space Sci. Rev.*, *215*(4), 31. doi: 10.1007/s11214-019-0599-5
- Sitnov, M. I., Buzulukova, N., Swisdak, M., Merkin, V. G., & Moore, T. E. (2013, January). Spontaneous formation of dipolarization fronts and reconnection onset in the magnetotail. *Geophys. Res. Lett.*, *40*, 22-27. doi: 10.1029/2012GL054701
- Sitnov, M. I., Guzdar, P. N., & Swisdak, M. (2003, July). A model of the bifurcated current sheet. *Geophys. Res. Lett.*, *30*, 45. doi: 10.1029/2003GL017218
- Sitnov, M. I., & Merkin, V. G. (2016, August). Generalized magnetotail equilibria: Effects of the dipole field, thin current sheets, and magnetic flux accumulation. *J. Geophys. Res.*, *121*, 7664-7683. doi: 10.1002/2016JA023001
- Sitnov, M. I., Merkin, V. G., Swisdak, M., Motoba, T., Buzulukova, N., Moore, T. E., . . . Ohtani, S. (2014, September). Magnetic reconnection, buoyancy, and flapping motions in magnetotail explosions. *J. Geophys. Res.*, *119*, 7151-7168. doi: 10.1002/2014JA020205
- Sitnov, M. I., & Schindler, K. (2010, April). Tearing stability of a multi-scale magnetotail current sheet. *Geophys. Res. Lett.*, *37*, 8102. doi: 10.1029/2010GL042961
- Sitnov, M. I., Sharma, A. S., Guzdar, P. N., & Yoon, P. H. (2002, September). Reconnection onset in the tail of Earth's magnetosphere. *J. Geophys. Res.*, *107*, 1256. doi: 10.1029/2001JA009148
- Sitnov, M. I., Stephens, G. K., Motoba, T., & Swisdak, M. (2021). Data Mining Reconstruction of Magnetotail Reconnection and Implications for Its First-Principle Modeling. *Front. Phys.*. doi: 10.3389/fphy.2021.644884

- Sitnov, M. I., Stephens, G. K., Tsyganenko, N. A., Miyashita, Y., Merkin, V. G., Motoba, T., ... Genestreti, K. J. (2019, Nov). Signatures of Nonideal Plasma Evolution During Substorms Obtained by Mining Multimission Magnetometer Data. *Journal of Geophysical Research (Space Physics)*, *124*(11), 8427-8456. doi: 10.1029/2019JA027037
- Sitnov, M. I., & Swisdak, M. (2011, December). Onset of collisionless magnetic reconnection in two-dimensional current sheets and formation of dipolarization fronts. *J. Geophys. Res.*, *116*, 12216. doi: 10.1029/2011JA016920
- Sitnov, M. I., Swisdak, M., & Divin, A. V. (2009, April). Dipolarization fronts as a signature of transient reconnection in the magnetotail. *J. Geophys. Res.*, *114*, A04202. doi: 10.1029/2008JA013980
- Sitnov, M. I., Swisdak, M., Guzdar, P. N., & Runov, A. (2006, August). Structure and dynamics of a new class of thin current sheets. *J. Geophys. Res.*, *111*, 8204. doi: 10.1029/2005JA011517
- Sitnov, M. I., Zelenyi, L. M., Malova, H. V., & Sharma, A. S. (2000, June). Thin current sheet embedded within a thicker plasma sheet: Self-consistent kinetic theory. *J. Geophys. Res.*, *105*, 13029-13044. doi: 10.1029/1999JA000431
- Somov, B. V., & Verneta, A. I. (1993, September). Tearing Instability of Reconnecting current Sheets in Space Plasmas. *Space Sci. Rev.*, *65*(3-4), 253-288. doi: 10.1007/BF00754510
- Speiser, T. W. (1965, September). Particle Trajectories in Model Current Sheets, 1, Analytical Solutions. *J. Geophys. Res.*, *70*, 4219-4226. doi: 10.1029/JZ070i017p04219
- Steinhauer, L. C., McCarthy, M. P., & Whipple, E. C. (2008, April). Multifluid model of a one-dimensional steady state magnetotail current sheet. *J. Geophys. Res.*, *113*, 4207. doi: 10.1029/2007JA012578
- Sturrock, P. A. (1966, August). Model of the High-Energy Phase of Solar Flares. *Nature*, *211*, 695-697. doi: 10.1038/211695a0
- Swisdak, M., Rogers, B. N., Drake, J. F., & Shay, M. A. (2003, May). Diamagnetic suppression of component magnetic reconnection at the magnetopause. *Journal of Geophysical Research (Space Physics)*, *108*(A5), 1218. doi: 10.1029/2002JA009726
- Tenerani, A., Velli, M., Pucci, F., Landi, S., & Rappazzo, A. F. (2016). 'ideally' unstable current sheets and the triggering of fast magnetic reconnection. *Journal of Plasma Physics*, *82*(5).
- Tenerani, A., Velli, M., Rappazzo, A. F., & Pucci, F. (2015, November). Magnetic Reconnection: Recursive Current Sheet Collapse Triggered by Ideal Tearing. *Astrophys. J. Lett.*, *813*, L32. doi: 10.1088/2041-8205/813/2/L32
- Terasawa, T., Shibata, K., & Scholer, M. (2000). Comparative Study of Flares and Substorms. *Advances in Space Research*, *26*, 573-583. doi: 10.1016/S0273-1177(99)01087-X
- Tsurutani, B. T., & Ho, C. M. (1999). A review of discontinuities and Alfvén waves in interplanetary space: Ulysses results. *Reviews of Geophysics*, *37*, 517-524. doi: 10.1029/1999RG900010
- Vasko, I. Y., Artemyev, A. V., Popov, V. Y., & Malova, H. V. (2013, February). Kinetic models of two-dimensional plane and axially symmetric current sheets: Group theory approach. *Physics of Plasmas*, *20*(2), 022110. doi: 10.1063/1.4792263
- Vasko, I. Y., Petrukovich, A. A., Artemyev, A. V., Nakamura, R., & Zelenyi, L. M. (2015, October). Earth's distant magnetotail current sheet near and beyond lunar orbit. *J. Geophys. Res.*, *120*, 8663-8680. doi: 10.1002/2015JA021633
- Verneta, A. I., & Somov, B. V. (1987, July). Stabilizing Effect of a Transverse Magnetic Field in Current Sheets of Solar Flares. *Soviet Astronomy Letters*, *13*, 302.
- Virtanen, P., Gommers, R., Oliphant, T. E., Haberland, M., Reddy, T., Courn-

- peau, D., ... others (2020). Scipy 1.0: fundamental algorithms for scientific computing in python. *Nature Methods*, 1–12.
- Walsh, A. P., Owen, C. J., Fazakerley, A. N., Forsyth, C., & Dandouras, I. (2011, March). Average magnetotail electron and proton pitch angle distributions from Cluster PEACE and CIS observations. *Geophys. Res. Lett.*, *38*, 6103. doi: 10.1029/2011GL046770
- Wang, C.-P., Zaharia, S. G., Lyons, L. R., & Angelopoulos, V. (2013, January). Spatial distributions of ion pitch angle anisotropy in the near-Earth magnetosphere and tail plasma sheet. *J. Geophys. Res.*, *118*, 244-255. doi: 10.1029/2012JA018275
- Wang, S., Lee, L., & Wei, C. (1988). Streaming tearing instability in the current sheet with a super-alfvenic flow. *The Physics of fluids*, *31*(6), 1544–1548.
- Yamada, M., Kulsrud, R., & Ji, H. (2010, January). Magnetic reconnection. *Reviews of Modern Physics*, *82*, 603-664. doi: 10.1103/RevModPhys.82.603
- Yoon, P. H., & Lui, A. T. Y. (2005, January). A class of exact two-dimensional kinetic current sheet equilibria. *J. Geophys. Res.*, *110*, 1202. doi: 10.1029/2003JA010308
- Zelenyi, L. M., Artemyev, A. V., Malova, H. V., & Popov, V. Y. (2008, February). Marginal stability of thin current sheets in the Earth’s magnetotail. *Journal of Atmospheric and Solar-Terrestrial Physics*, *70*, 325-333. doi: 10.1016/j.jastp.2007.08.019
- Zelenyi, L. M., Dolgonosov, M. S., Perroomian, V., & Ashour-Abdalla, M. (2006, September). Effects of nonlinearity on the structure of PSBL beamlets. *Geophys. Res. Lett.*, *33*, L18103. doi: 10.1029/2006GL026176
- Zelenyi, L. M., Malova, H. V., Artemyev, A. V., Popov, V. Y., & Petrukovich, A. A. (2011, February). Thin current sheets in collisionless plasma: Equilibrium structure, plasma instabilities, and particle acceleration. *Plasma Physics Reports*, *37*, 118-160. doi: 10.1134/S1063780X1102005X
- Zelenyi, L. M., Malova, H. V., Popov, V. Y., Delcourt, D. C., Ganushkina, N. Y., & Sharma, A. S. (2006, March). “Matreshka” model of multilayered current sheet. *Geophys. Res. Lett.*, *33*, 5105. doi: 10.1029/2005GL025117
- Zhou, X., Angelopoulos, V., Runov, A., Sitnov, M. I., Coroniti, F., Pritchett, P., ... Glassmeier, K. (2009, March). Thin current sheet in the substorm late growth phase: Modeling of THEMIS observations. *J. Geophys. Res.*, *114*, 3223. doi: 10.1029/2008JA013777